PHYSICAL REVIEW C VOLUME 5, NUMBER 2 FEBRUARY 1972

Study of the 2p-1h Structure of ^{17}O via the ^{15}N(^{3}He,p) Reaction

M.-C. Lemaire and M. C. Mermaz
Centre d'Etudes Nucléaires de Saclay, Gif-sur-Yvette, France

and

Kamal K. Seth
*Northwestern University, Evanston, Illinois,**
and Centre d'Etudes Nucléaires de Saclay, Gif-sur-Yvette, France

(Received 6 July 1971)

The double-stripping reaction ^{15}N(^{3}He,p)^{17}O has been studied with a magnetic spectrograph at an incident ^{3}He energy of 18 MeV, with an energy resolution of about 30 keV. Differential cross sections have been measured for transitions to states in ^{17}O up to an excitation energy of 11 MeV. The data have been analyzed in the distorted-wave Born approximation using the Glendenning formalism and the multishell shell-model wave functions of Zuker, Buck, and McGrory for states in ^{17}O. The model wave functions are found to fit the data quite well for a number of low lying-states. However, several exceptions are also found.

1. INTRODUCTION

There is now a considerable body of both experimental and theoretical evidence which suggests that ground states of even the doubly magic nuclei, such as ^{16}O, ^{40}Ca, and ^{208}Pb, contain appreciable correlations in the form of 2p-2h, 4p-4h, etc. components, in addition to the hopefully predominant 0p-0h configuration. (The particles and holes are counted from the Fermi level of the idealized, independent-particle shell model.) For ^{16}O the correlated particles may be expected to exist mainly in the $2s$-$1d$ shells and the holes in the $1p$ shell. Thus, in ^{17}O the negative-parity states may be expected to have mainly 2p-1h and 4p-3h components. Direct reactions involving transfer of m particles on a target nucleus $(A-n)$ preferentially populate those states of the residual nucleus $(A+m-n)$ which have parentage in the ground state of the target nucleus $(A-n)$. By suitable choice of the direct reaction and the target nucleus $(A-n)$ we can therefore preferentially excite and study m-particle–n-hole components in the states of the final nucleus $(A+m-n)$. In the positive-parity states of ^{17}O we may thus study mainly neutron single-particle components with the ^{16}O(d,p) reaction, 3p-2h components with the ^{14}N(α,p) reaction, and 5p-4h components with the ^{12}C(^{6}Li,p) or ^{12}C(^{7}Li,d) reactions. Similarily, in the negative-parity states we may study 2p-1h components with the ^{15}N(α,d) or ^{15}N(^{3}He,p) reactions, and 4p-3h components with the ^{13}C(^{7}Li,t) reaction, for example (provided, of course, all these reactions proceed by a direct mechanism). (More complicated components of states in ^{17}O are also excited in each of these reactions, but only via the weaker, correlated part of the ground-state wave function of the target nuclei.) Because of characteristic coherence effects, in many-particle-transfer reactions one cannot obtain spectroscopic amplitudes directly, but can only test amplitudes provided by theoretical calculations. In this paper we report on our study of the double-stripping reaction ^{15}N(^{3}He,p)^{17}O, in order to test theoretical model wave functions which have recently become available for states in ^{17}O.

The reaction ^{15}N(^{3}He,p)^{17}O was first studied by Seth *et al.*[1] and Seth, Miller, and Biggerstaff[2] at incident ^{3}He energies of 7 and 10 MeV. While qualitative conclusions about strong excitation of $T=\frac{1}{2}$ states at 5.7, 7.4, 7.7, 8.5, 8.9, and 9.1 MeV and the $T=\frac{3}{2}$ analogous state at 11.0 MeV could be drawn from these data, the experimental results were largely inconclusive. Because of the use of a gaseous target, energy resolution was of the order of 60 keV and data were confined to $\theta>20°$. The incident energy was also not high enough to insure that the direct-reaction mode was dominant. Recently two other attempts at studying this reaction at higher energies have been made, but no detailed reports have been given.[3,4] The analogous reaction (for $T=\frac{1}{2}$ states only), ^{15}N(α,d), was earlier studied by Harvey and co-workers[5-7] as a part of their systematic study of states of the $(d_{5/2})^2_{J=5}$ configuration throughout the s-d shell. The latest of these experiments[7] was done at $E_\alpha=45.4$ MeV with an energy resolution of about 150 keV. No attempt at testing model wave functions was made. The present (^{3}He,p) experiment at $E(^3\text{He})=18$ MeV, with an energy resolution of about 30 keV, was motivated by the desire to remove the shortcomings of the experiments of Seth *et al.*[1,2] and to test theoretical wave functions for states of ^{17}O by the dis-

torted-wave Born-approximation (DWBA) analysis of the differential cross sections for this double-stripping reaction.

2. THEORETICAL CALCULATIONS OF ^{17}O

The theoretical calculations of the structure of ^{17}O have all been based on certain clear-cut empirical facts. From the (d,p) experiments (see, for example, Naqib and Green[8]) it is known that the major part of the single-particle strength of the $d_{5/2}$ and $s_{1/2}$ orbits lies in the $\frac{5}{2}^+$ ground state and the $\frac{1}{2}^+$ first excited state at 0.874 MeV ($S=0.8$ to 1.0). The $d_{3/2}$ orbit lies about 6 MeV higher and, from neutron scattering experiments,[9] it is found that a major part of the $d_{3/2}$ single-particle strength indeed lies in the two $\frac{3}{2}^+$ states at 5.081 and 7.294 MeV ($\sum S \simeq 0.7$). The low-lying negative-parity levels are very weakly excited in (d,p) and neutron scattering experiments, indicating that $p_{1/2}$ and $p_{3/2}$ hole components in the target wave functions are not too large. [The $\frac{1}{2}^-$ state at 3.053 MeV, for example, has a (d,p) spectroscopic strength $(2J+1)C^2S \simeq 0.06$, indicating that the $p_{1/2}$ hole component in the ^{16}O(g.s.) wave function has an amplitude of the order of only 0.18.] On the other hand, the manifestations of collective features of the nuclei in the sd shell are also quite well known and it is quite evident that the particle-hole excitations must play a significant role in the structure of the excited states.

The importance of particle-hole excitations in the sd-shell nuclei was first pointed out in 1954 by Christy and Fowler,[10] who concluded that the 3.053-MeV ($\frac{1}{2}^-$) state in ^{17}O must contain substantial parts of 4p-3h components. Since then several calculations have been reported in the literature[11-22] which take into account, to a varying degree and in different approximations, particle-hole components. Of the many calculations, only the last, namely the one due to Zuker, Buck, and McGrory[20] (ZBM), provides sufficiently detailed wave functions for both positive- and negative-parity states to be of direct usefulness in our analysis of two-nucleon-transfer angular distributions. We describe these various calculations briefly in order to place the work of ZBM in proper perspective.

Harvey[11] calculated the negative-parity states in ^{17}O with a $1p$ particle excited from the closed ^{16}O core into the $2s$-$1d$ shell, i.e., as 2p-1h states in the SU_3 coupling scheme. He concluded that the lowest $\frac{1}{2}^-$ state at 3.053 MeV was most likely not a 2p-1h state, and that the second $\frac{1}{2}^-$ state at 5.938 MeV was the state predicted by his calculations. No other details of the calculations were given. Ripka[12] considered a weak-coupling model in which the negative-parity states were considered as a valence particle coupled to the negative-parity particle-hole states of ^{16}O. He concluded that a more successful approach was that of coupling a $p_{1/2}$ hole to the positive-parity states of ^{18}O which were considered as states of two particles in the sd shell. Margolis and Takacsy[13] made a detailed 2p-1h calculation. Even-parity states for the $A=18$ nuclei were constructed with two particles in $d_{5/2}$, $s_{1/2}$, and $d_{3/2}$ orbits, and the negative-parity states of $A=17$ nuclei were obtained by coupling a $p_{1/2}$ hole to them. Brown[14] pointed out that since 4p-4h components in ^{16}O(g.s.) are as important as 2p-2h components, pure 2p-1h calculations of negative-parity states may not be realistic. Brown and Green[15] and Shukla and Brown[16] calculated the even-parity and odd-parity states of ^{17}O by mixing spherical shell-model states with deformed states obtained by promoting two and four particles from the $p_{1/2}$ shell to the $s_{1/2}, d_{5/2}$ shells. Very recently the detailed work of Ellis and Engeland[17] has become available in which Brown's original objection is removed, since both 2p-1h and 4p-3h excitation are considered. Since the configuration basis was limited by choosing the SU_3 scheme, the full sd and p shells could be considered, i.e., holes in the $p_{3/2}$ shell and particles in the $d_{3/2}$ shell were allowed in addition to the orbits usually considered active, $p_{1/2}$, $d_{5/2}$, and $s_{1/2}$.

The last calculation, already referred to, is the "exact" multishell shell-model calculation of ZBM.[18-20] In this calculation the problem of five particles in three orbits $1p_{1/2}$, $2s_{1/2}$, and $1d_{5/2}$ was solved exactly and detailed wave functions for four lowest states of each $J\pi T$ were given. We shall discuss this calculation in detail later. At this point it is sufficient to notice that $d_{3/2}$, $p_{3/2}$ shells were not considered active in this calculation, because the dimensionality of the problem makes the inclusion of these orbits impossible in the "exact" calculation.

Recently, Wildenthal and McGrory[21] (WM) have attempted to optimize the parameters of the "exact" multishell shell-model calculation for the $A=13$ to 20 region and preliminary results of these calculations have become available.[21] In most cases the (WM) wave functions differ very slightly from the ZBM[20] wave functions.

It was noticed by Margolis and Takacsy that 2p-1h states do not come down low enough to explain the experimental spectrum of negative-parity states. Bobker[22] has shown explicitly that 4p-3h admixtures lower the energy of most levels by 2 to 3 MeV. These results have been further confirmed by ZBM and Ellis and Engeland. For this reason we have listed in Table I results of only those calculations in which both 2p-1h and 4p-3h excitations were considered. Some salient fea-

tures in Table I are the following:

For the $\frac{5}{2}^+$ and $\frac{1}{2}^+$ states the results of Brown and Green based on their semiempirical model are indeed very similar to those of Ellis and Engeland. ZBM (and WM) generally have about 10% smaller single-particle components and about 10% larger 3p-2h components. For the first $\frac{3}{2}^+$ state at 5.081 MeV, which is known experimentally to have substantial single-particle strength, and for which Brown and Green do find a large single-particle amplitude, there is no counterpart in the ZBM calculations, since the $d_{3/2}$ orbit was not considered active. The first $\frac{3}{2}^+$ state of the ZBM calculation has, however, a structure quite similar to Brown and Green's second $\frac{3}{2}^+$ state (except, of course, for the single-particle component).

For the negative-parity states the agreement between the results of the different calculations is not as good. For the $\frac{1}{2}^-$ and $\frac{3}{2}^-$ states the results of Shukla and Brown[16] and Ellis and Engeland[17] are in reasonable agreement, but the differences between these and the ZBM (and WM) results are sub-

TABLE I. Particle-hole nature of wave functions for $T=\frac{1}{2}$ states in ^{17}O according to various authors. For the complete wave function according to Zuker, Buck, and McGrory, see Table IV. In most cases wave functions for the first two states of each J^π are given, the second one being in parentheses. The p-h components given here were in many cases calculated from the detailed wave functions given by authors. They do not account for 100% of the wave function, because individual components with amplitudes ≤ 0.25 were often neglected by the authors themselves.

J^π	E_{exp} (MeV)	E_{theor} (MeV)	Author	1p-0h	3p-2h	5p-4h
$\frac{5}{2}^+$	0	0	Brown (Ref. 15)	0.90	0.41	0.08
		0	Ellis (Ref. 17)	0.92	0.39	
		0	Zuker (Ref. 20)	0.82	0.52	0.17
		0	Wildenthal (Ref. 21)	0.82	0.49	0.17
$\frac{1}{2}^+$	0.874	0.50	Brown	0.88	0.46	0.11
			Ellis	0.87	0.49	
		0.83	Zuker	0.78	0.58	0.21
		0.85	Wildenthal	0.78	0.60	0.19
$\frac{3}{2}^+$	5.081 (5.873)	5.10 (5.82)	Brown	0.72 (0.26)	0.52 (0.49)	0.47 (0.83)
		5.28	Zuker		0.63	0.78
		4.88	Wildenthal		0.49	0.74
				2p-1h	4p-3h	
$\frac{1}{2}^-$	3.053 (5.938)		Shukla (Ref. 16)	0.90 (0.43)	0.43 (0.90)	
		3.1 (6.3)	Ellis	0.81 (0.62)	0.58 (0.78)	
		2.88 (5.74)	Zuker	0.63 (0.74)	0.79 (0.41)	
		3.27 (6.21)	Wildenthal	0.49 (0.81)	0.83 (0.55)	
$\frac{3}{2}^-$	4.549 (5.381)		Shukla	0.87 (0.49)	0.49 (0.87)	
		4.9 (6.1)	Ellis	0.88 (0.66)	0.47 (0.75)	
		4.51 (5.41)	Zuker	0.79 (0.41)	0.41 (0.37)	
		4.62 (5.80)	Wildenthal	0.64 (0.81)	0.70 (0.46)	
$\frac{5}{2}^-$	3.845 (5.731?)[a]		Shukla	0.41 (0.91)	0.91 (0.42)	
		5.3 (7.7)	Ellis	0.82	0.57	
		3.48 (5.85)	Zuker	0.73 (0.72)	0.44 (0.43)	
		3.67 (6.27)	Wildenthal	0.72 (0.73)	0.60 (0.42)	
$\frac{7}{2}^-$	5.698 (7.687)	6.4 (8.2)	Ellis	0.92	0.38	
		5.62 (8.01)	Zuker	0.85 (0.79)	0.35 (0.41)	
		6.02 (8.08)	Wildenthal	0.87 (0.76)	0.32 (0.53)	
$(\frac{9}{2}^-)$	5.215?[b] (9.16)	6.7 (9.1)	Ellis	0.95 (0.93)	0.33 (0.35)	
		4.79 (7.09)	Zuker	0.84 (0.88)	0.27 (0.37)	
		5.39 (9.08)	Wildenthal	0.83 (0.87)	0.45 (0.40)	
$\frac{11}{2}^-$	7.74	7.3	Ellis	0.96	0.25	
		6.00	Zuker	0.89	0.41	
		7.23	Wildenthal	0.88	0.44	

[a] The second $\frac{5}{2}^-$ state predicted at about 6 MeV has not yet been definitely identified. The known $\frac{5}{2}^-$ state at 7.162 MeV most likely corresponds to the fourth $\frac{5}{2}^-$ state predicted by Zuker *et al.* at 7.97 MeV and by Wildenthal and McGrory at 7.85 MeV.

[b] The first $\frac{9}{2}^-$ state has not yet been experimentally identified. See Sec. 5 for discussion.

stantial. For the $\frac{5}{2}^-$ states the differences between Shukla and Brown[16] and others are most pronounced. As a matter of fact, for some of these states, e.g., the second $\frac{3}{2}^-$ state at 5.381 MeV, there are important differences between the ZBM and WM results. This fact emphasizes the sensitive character of these states. The agreement between the results of Ellis and Engeland and those of ZBM (and WM) improves with increasing J, i.e., as the number of available configurations becomes smaller. We will return to a more detailed discussion of some of these wave functions later, in Sec. 5.

3. EXPERIMENTAL PROCEDURE

The EN tandem Van de Graaff at Centre d'Etudes Nucléaires de Saclay provided a beam of doubly charged 18-MeV ^{3}He particles. The ^{15}N target used was made by evaporation of melamine $(CN_2H_2)_n$ enriched to about 99% in ^{15}N, on a 20-μg/cm^2 carbon foil. Measurement of the energy loss of 6.0498- and 6.0897-MeV α particles from a ^{212}Bi source gave the thickness of ^{15}N to be 25 ± 3 μg/cm^2, under the assumption that the deposited material was still in the chemical form $(CN_2H_2)_n$. The reaction protons were analyzed with a magnetic spectrograph and detected in Ilford K5 nuclear photographic emulsions. Deuterons and α particles from the (^{3}He, d) and (^{3}He, α) reactions were absorbed in a 100-μm-thick nickel absorber placed in front of the photographic plates. Beam current was integrated in the scattering chamber. A solid-state monitor counter, mounted within the chamber at 90° to the incident beam provided a continuous measure of elastic scattering from ^{15}N, and thus provided a check on beam integration and target stability.

The photographic plates were scanned in $\frac{1}{4}$-mm swaths; the scanning was partially done at Saclay and partially at the University of Bordeaux. Data were taken at 5° intervals from $\theta_{lab} = 5$ to 70°. Figure 1 shows a typical proton spectrum obtained at $\theta_{lab} = 20°$. The energy resolution [full width at half maximum (FWHM)] is seen to be about 30 keV.

Since proton groups from reactions ^{12}C(^{3}He, p)^{14}N begin to interfere with proton groups from the reaction ^{15}N(^{3}He, p)^{17}O for ^{17}O excitation energies above 3.85 MeV, considerable care had to be exercised in kinematically tracking ^{17}O groups through various angles of observation. Unambiguous identification of ^{17}O groups was made in this manner at nearly all the angles. The energies of the states excited in the present experiment, together with energies and J^π measured in other experiments are listed in Table II.

As indicated in Table II precision determination of energies of states in ^{17}O comes from three main sources: for excitation energies below 6 MeV, from the (d, p) experiments of Brown[23]; for excitation energies above 4.5 MeV, from the neutron

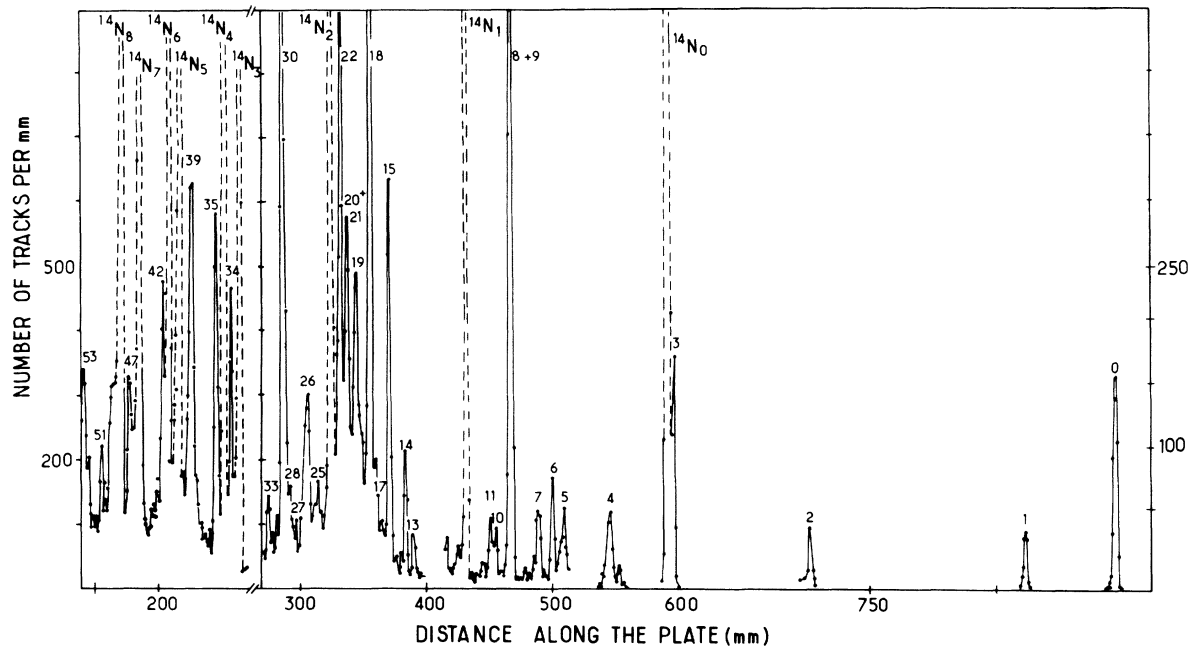

FIG. 1. Proton energy spectrum for the reaction ^{15}N(^{3}He,p)^{17}O. $E(^3\text{He}) = 18$ MeV, $\theta_{lab} = 20_0$, $B = 10^4$ G. The numbers correspond to energy levels in ^{17}O as listed in Table II. Peaks corresponding to the reaction ^{12}C(^{3}He,p)^{14}N are shown with dashed lines. The integrated charge is 1440 μC.

TABLE II. Excitation energies [with errors, $\pm\epsilon$ (keV)] and l, L, or J^π for states in ^{17}O.

No.	^{15}N(^{3}He, p) [a] (this expt) E^* (MeV) $\epsilon \leq 10$	L	^{15}N(α, d) (Ref. 7) E^* (MeV) $30 \leq \epsilon \leq 50$	^{16}O + n [b] (Refs. 9, 24, 25) E^* (MeV) $5 \leq \epsilon \leq 10$	J^π	^{16}O(d, p) (Ref. 23) E^* (MeV) $5 \leq \epsilon \leq 10$	l	J^π [c]	$\Gamma_{c.m.}$ (keV) ^{16}O + n	^{13}C + α
0	0	(1+3)	0			0	2	$\frac{5}{2}^+$		
1	0.874	1	0.87			0.871	0	$\frac{1}{2}^+$		
2	3.053	0				3.055	1	$\frac{1}{2}^-$		
3	3.845	2	3.85			3.846	3	$\frac{5}{2}^-$		
4	4.549	0	4.57	4.558	$\frac{3}{2}^-$	4.553	1	$\frac{3}{2}^-$	45	
5	5.081	(1)		5.083	$\frac{3}{2}^+$	5.083	2	$\frac{3}{2}^+$	94	
6	5.215	(4)	5.21	···		5.215		$(\frac{9}{2}^-)$*	<8	
7	5.381	0		5.377	$\frac{3}{2}^-$	5.378		$\frac{3}{2}^-$	41	
8	5.698	2	5.69	5.696	$\frac{7}{2}^-$	5.695		$\frac{7}{2}^-$	3.4	
9	···	(2)		5.731		5.731		$(\frac{5}{2}^-)$*	<1	
10	5.873	(1)		5.867	$\frac{3}{2}^+$	5.866		$\frac{3}{2}^+$	6.6	
11	5.938	0		5.936	$\frac{1}{2}^-$	5.940		$\frac{1}{2}^-$	24.5	
12	6.37			6.356	$\frac{1}{2}^+$			$\frac{1}{2}^+$	135	
13	6.861	(0)		6.859				$(\frac{1}{2}^-)$*	<1	
14	6.973	(1+3)		6.970				$(\frac{5}{2}^+)$*	<1	
						^{13}C + α (Refs. 26, 27) $\epsilon \leq 10$	J^π			
15	7.162	2		7.164	$\frac{5}{2}^-$	7.168	$\frac{5}{2}$	$\frac{5}{2}^-$	1.4	2.7
16	···			7.294	$\frac{3}{2}^+$			$\frac{3}{2}^+$	500	
17	···			7.377	$\frac{5}{2}^+$			$\frac{5}{2}^+$	0.5	≤2
18	7.382	2	7.37	7.380	$\frac{5}{2}^-$	7.380	$\frac{5}{2}$	$\frac{5}{2}^-$	1.1	
19	7.561			···	···	7.573	$\geq\frac{7}{2}$	$(\frac{7}{2}^+)$*		≤4
20	···			7.67	$\frac{3}{2}^-$	···		$\frac{3}{2}^-$	405	
21	7.687			7.684	$\frac{7}{2}^-$	7.685	$\geq\frac{5}{2}$	$\frac{7}{2}^-$	14	22
22	7.761	4	7.74	···	···	···		$(\frac{11}{2}^-)$*		
23	7.938			7.91	$\frac{1}{2}^-$	7.97	$\frac{1}{2}^-$	$\frac{1}{2}^-$	69	80
24				7.96	$\frac{1}{2}^+$	···		$\frac{1}{2}^+$	~80	
25	8.054	(1)		8.07	$\frac{3}{2}^+$	8.064	$\frac{3}{2}^+$	$\frac{3}{2}^+$	82	70
26	8.192	0	8.15	8.21	$\frac{3}{2}^-$	8.197	$\frac{3}{2}^-$	$\frac{3}{2}^-$	62	70
27	8.322			8.33		8.332	$\frac{1}{2}^+$	$\frac{1}{2}^+$	<5	10
28	8.390			8.40	$\frac{5}{2}$	8.393	$\frac{5}{2}^+$	$\frac{5}{2}^+$		4
29	···			8.47	$\geq\frac{3}{2}$	8.460	$\frac{7}{2}^+$	$\frac{7}{2}^+$		7

TABLE II *(Continued)*

No.	^{15}N(^{3}He, p) [a] (this expt) E^* (MeV) $\epsilon \leq 10$	L	^{15}N(α, d) (Ref. 7) E^* (MeV) $30 \leq \epsilon \leq 50$	^{16}O + n [b] (Refs. 9, 24, 25) E^* (MeV) $5 \leq \epsilon \leq 10$	J^π	^{16}O(d, p) (Ref. 23) E^* (MeV) $5 \leq \epsilon \leq 10$	l	J^π [c]	$\Gamma_{c.m.}$ (keV) ^{16}O + n	$\Gamma_{c.m.}$ (keV) ^{13}C + α
30	8.492	(2)	8.46	8.51	$\geq\frac{3}{2}$	8.498	$\frac{5}{2}^-$	$\frac{5}{2}^-$		5
31	8.682			8.69	$\frac{3}{2}$	8.679	$\frac{3}{2}^-$	$\frac{3}{2}^-$	55	50
32	...			...	...	8.873	$\frac{3}{2}^+$	$\frac{3}{2}^+$		100
33	8.900		8.89	...	...	8.884	$\frac{7}{2}^-$	$\frac{7}{2}^-$		6
34	8.955			8.96	$\frac{7}{2}$	8.945	$\frac{7}{2}^-$	$\frac{7}{2}^-$	28	20
35	...			...		9.14	$\frac{1}{2}^-$	$\frac{1}{2}^-$		4
36	9.16	(4)	9.14	9.18	$\geq\frac{3}{2}$	9.18	$\frac{7}{2}^-$	$(\frac{9}{2}^-)$	$\leq$17	3
37	...			...	...	9.20	$\frac{5}{2}^+$	$\frac{5}{2}^+$		5
38	...			9.45	$\geq\frac{3}{2}$	...		$\geq\frac{3}{2}$	140	
39	9.495			...	...	9.50	$\frac{5}{2}^-$	$\frac{5}{2}^-$		15
40	9.712			9.705	$\geq\frac{5}{2}$	9.72	$\frac{7}{2}^+$	$\frac{7}{2}^+$	28	16
41				9.79	$\geq\frac{3}{2}$	9.74	$\frac{3}{2}^+$	$\frac{3}{2}^+$	28	61
42	9.856		9.81	9.87	$\geq\frac{1}{2}$	9.86	$\frac{3}{2}^+$	$\frac{3}{2}^+$	25	12
43				...	...	9.95	$\frac{7}{2}^+$	$(\frac{7}{2}^+)$		107
44				...	...	10.14	$\frac{5}{2}^+$	$\frac{5}{2}^+$		138
			^{13}C(α, n) (Ref. 29)							
45				10.158	$\geq\frac{3}{2}$	10.17	$\frac{7}{2}^-$	$\frac{7}{2}^-$		46
46	(10.24)					10.24	$\frac{7}{2}^+$	$\frac{7}{2}^+$		122
47	10.33					10.33	$(\frac{7}{2}^-)$	$(\frac{7}{2}^-)$		
48			10.423			10.4				<20
49						10.49	$(\frac{5}{2})$	$(\frac{5}{2})$		75
50	10.57		10.560	10.545	$\geq\frac{3}{2}$	10.58	$(\frac{5}{2}, \frac{7}{2})$	$(\frac{5}{2}, \frac{7}{2})$		45
51	10.693		...			10.70	$(\frac{7}{2}^+)$	$(\frac{7}{2}^+)$		$\leq$25
52	10.782		10.770			10.79	$(\frac{5}{2})$	$(\frac{5}{2})$		75
53	10.913		10.903	10.915	$\geq\frac{3}{2}$	10.92	...			60
54	11.032		11.027	...	...	11.05	...			45
55	11.075		...	...	...	...	...	$\frac{1}{2}^-$ ($T=\frac{3}{2}$)		5

[a] Values of L are indicated in parentheses for those cases in which either the DWBA fits with the indicated L (based on ZBM wave functions) are poor, or in which the dominant L has been obtained by visual examination of data only.

[b] The authors of Ref. 9 have, subsequent to publication, withdrawn a proposed $\frac{3}{2}^+$ level at 7.691 MeV. They have found a new $\frac{1}{2}^+$ level at $\approx$7.96 MeV.

[c] Values of spin marked with asterisks have not been directly measured and are still speculative. They are based only on the arguments given in this paper. For levels at 7.761 and 9.16 MeV the same assignments were earlier given by LZH (Ref. 7).

total and scattering cross-section measurements[9,24,25] on ^{16}O; and for excitation energies above 7 MeV from α elastic and nonelastic experiments[26-29] on ^{13}C. In regions of overlap, results from these various experiments are generally in good agreement. While many other experiments exist in literature in which states of ^{17}O are excited over a wide range of energies,[30-32] these experiments generally do not have comparable precision in energy determination. In the present ($^3He, p$) experiments a majority of states between the ground state and 10-MeV excitation are excited and we are able to quote their energies with errors less than ±10 keV. In general, agreement with results of other experiments of comparable accuracy is excellent. We mention below some of the exceptions.

An excited state was reported at 6.24 MeV in early 1951 (d, p) experiments of Burrows and Powell.[33] This state has not been observed in any other subsequent experiment, including ours. We do not believe that it exists and have not included it in Table II. Further, we believe that there is a systematic discrepancy in the energies quoted by Lu, Zisman, and Harvey (LZH)[7] from their (α, d) experiments. Above 6 MeV their energies are consistently lower, and by 9-MeV excitation the difference is nearly 40 keV. Errors of this magnitude are, however, still within the errors quoted by these authors.

Above 7-MeV excitation our energies are generally between 5 and 15 keV lower than those reported by the (α, n) experiments. This trend, though well within quoted errors, had to be kept in mind in establishing correspondence between the levels observed in the two experiments. Most of the levels seen in $^{16}O + n$ and $^{13}C + \alpha$ experiments are also seen in our ($^3He, p$) experiment. Several of the states could not be identified, because of their exceptionally large width [e.g., states at 7.294 MeV ($\Gamma = 500$ keV), and 7.67 MeV ($\Gamma = 405$ keV)], while several others (e.g., states at 5.731, 7.377, 8.460, 8.873, 9.14, and 9.20 MeV) could not be resolved separately, since they are parts of close doublets and triplets.

Transitions to nearly all known states below 9.2 MeV have been observed in the predominantly compound-nuclear reactions $^{13}C(^6Li, p)$ and $^{13}C(^7Li, t)$ and in the semidirect reaction $^{13}C(^6Li, d)$, but the energy resolution in these experiments was much poorer and these are not included in Table II. The 7.761-MeV state, which is strongly populated in both ($^3He, p$) and (α, d) experiments has not been served in $^{16}O + n$ or $^{13}C + \alpha$ experiments. This might be indicative of its almost pure 2p-1h, $[(d_{5/2})^2_{J=5} p_{1/2}{}^{-1}]_{11/2^-}$ nature, as suggested by Harvey *et al.*[5-7] This is, however, not true for the 9.16-MeV state, which is suggested by the same authors to be the corresponding $\frac{9}{2}^-$ state, $[(d_{5/2})^2_{J=5} p_{1/2}{}^{-1}]_{9/2^-}$. If this is true the spin deter-

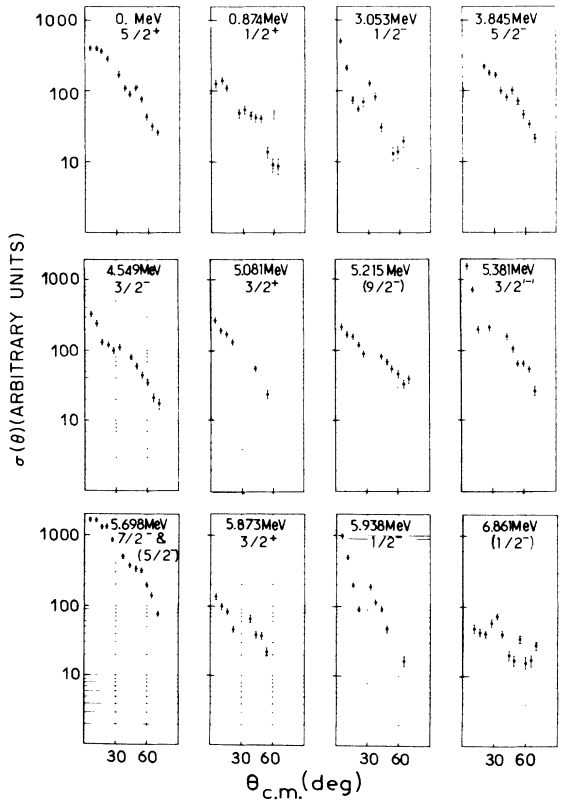

FIG. 2. Differential cross sections in units of 0.27 ±0.05 μb, for transitions identified in this experiment.

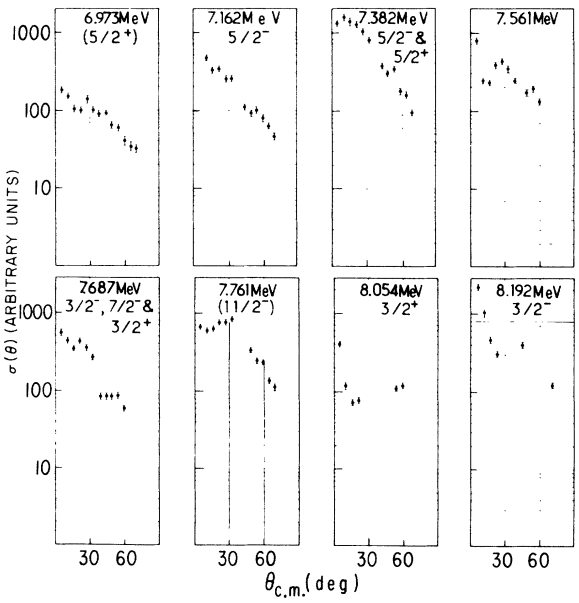

FIG. 3. Differential cross sections in units of 0.27 ±0.05 μb, for transitions identified in this experiment.

mination $\frac{7}{2}^-$ from $^{13}C(\alpha,n)$ experiment of Kerr *et al.*[27] must be in error. In a recent polarization measurement of $^{13}C(\alpha,n)$ reaction, Baker *et al.*[28] find agreement with the spin determinations of Kerr *et al.*[27] except for the following cases: These authors suggest a doublet at 8.68 MeV with spins $\frac{3}{2}^-$, $\frac{1}{2}^-$; a new state at 9.65 MeV with spin $\frac{3}{2}^-$; and a change in the spin of 9.95-MeV state from $\frac{7}{2}^+$ to $\frac{5}{2}^+$.

The two highest-energy levels excited in the present experiment are those at 11.032 ± 0.004 and 11.075 ± 0.004 MeV. The latter of these is definitely the $T=\frac{3}{2}$, $J=\frac{1}{2}^-$ analog of the ^{17}N ground state, which was first identified in the experiments of Seth *et al.*[2] Its energy was determined as 11.075 ± 0.005 MeV by Barnes *et al.*[34] by means of ^{15}N-($^3He,p$) reaction and as 11.082 ± 0.006 MeV by Detraz and Duhm[35] by means of $^{18}O(^3He,\alpha)$ reaction.

Relative differential cross sections measured for transitions of each of the 29 states in ^{17}O are shown in Figs. 2–4. Using our measurement of target thickness (error < ± 15%), integrated charge (error < ± 5%), and solid angle of the spectrograph (error < ± 5%), absolute cross sections for the observed transitions could be obtained with an estimated error of less than ±20%. These are shown in Figs. 10 through 15 in Sec. 5.

In a separate experiment done in a scattering chamber with a solid-state detector, the 18-MeV ^3He elastic scattering angular distribution was

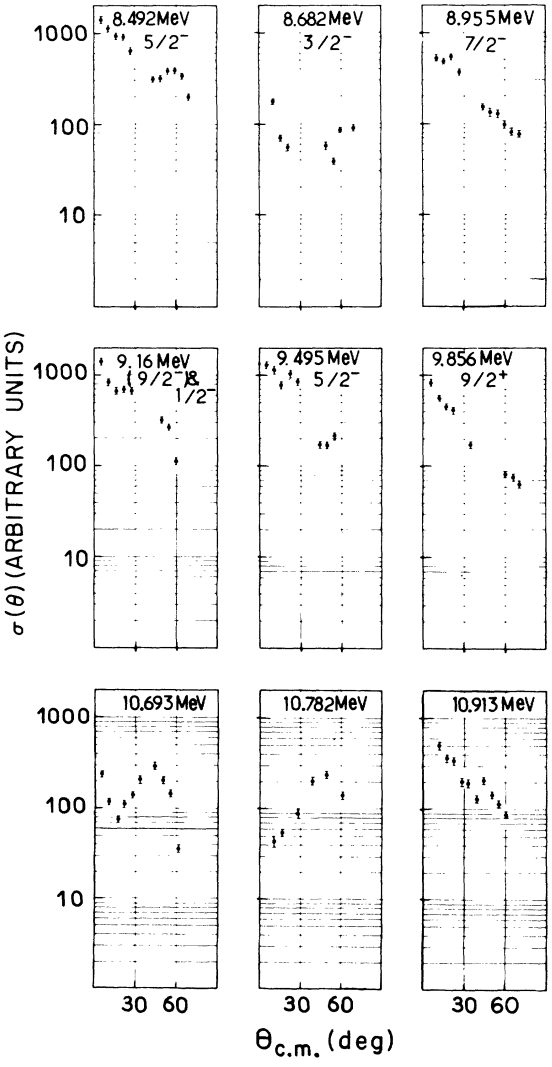

FIG. 4. Differential cross sections in units of 0.27 ± 0.05 μb, for transitions identified in this experiment.

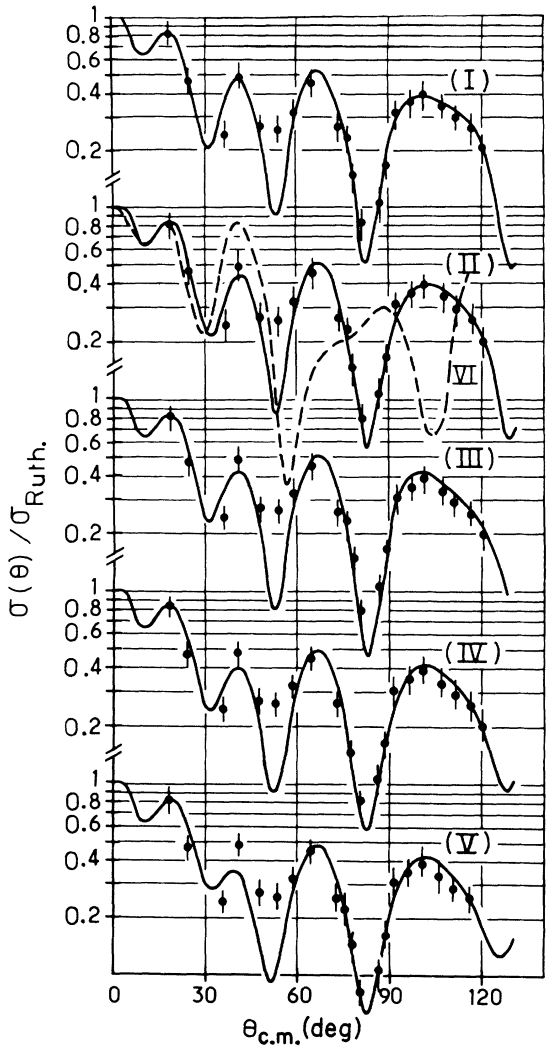

FIG. 5. $\sigma(\theta)/\sigma(\theta)_{RUTH}$ for elastic scattering of 18-MeV ^3He particles by ^{15}N. Curves correspond to results of optical-model calculations. The Roman numerals in parentheses refer to the different sets of optical-model parameters in Table III. Notice the extremely poor fit provided by Set VI.

measured between 15 and 105°. The measured cross sections, expressed as $\sigma(\theta)/\sigma_R(\theta)$ are shown in Fig. 5.

4. OPTICAL-MODEL ANALYSIS OF ELASTIC SCATTERING

As is well known, in order to make a DWBA analysis of the reaction data one needs the parameters of the distorting potentials in both the entrance and exit channels of the reaction. This potential is assumed to be the optical potential which describes elastic scattering in these channels.

From earlier work on two-nucleon-transfer reactions, it is known that differential cross sections for these reactions depend rather critically on the optical-potential parameters in the entrance channel. For this reason, as already mentioned, we have measured elastic scattering angular distributions for the scattering of 18-MeV ^{3}He particles by ^{15}N. These data have been analyzed for the search of best-fit optical-potential parameters.

It is well known that the best-fit optical-potential parameters show definite ambiguities, both discrete (when the product $V_0r_0^2$ assumes different discrete values which are approximate multiples of a constant) and continuous (when V_0 and r_0 vary to keep the product $V_0r_0^2$ constant). In our analysis we find this to be the case. In Table III we list five sets of parameters which give almost equally good fits to our elastic scattering data, as shown in Fig. 5. If we express the product $V_0r_0^2 = 85n$ MeV fm^2, we find that (within ±10%) Set V belongs to $n=1$, Set IV to $n=2$, Sets II and III to $n=3$, and Set I to $n=4$. It is generally accepted that the depth of the real part of the optical potential for a composite "particle" of mass 3 should be approximately three times the depth of the corresponding potential for nucleons. In terms of the product $V_0r_0^2$ this criterion corresponds to Sets II and III which do show somewhat better fits to the data for $\theta \leq 70°$ than either of the Sets IV and V, although χ^2 values over the whole angular range show no such clearcut preference. Set VI, whose origin will be discussed later, gives a very poor fit to the data.

In order to see how much the choice of ^{3}He potentials affects the (^{3}He, p) angular distributions, we have calculated angular distributions for two transitions using the various potentials of Table III for ^{3}He, and proton optical-potential parameters based on Perey's systematic study[36] of proton scattering. These are shown in Fig. 6. The dominant (2p-1h) components in the 3.053-MeV ($\frac{1}{2}^-$) state are $(d)^2_{L=J=0}$ and $(s)^2_{L=J=0}$ coupled to the $\frac{1}{2}^-$ ^{15}N core (see Sec. 5); this transition is, therefore, expected to be essentially pure $L=0$. Similarly, the 3.845-MeV ($\frac{5}{2}^-$) state is mainly two sd nucleons coupled to $L=J=2$ with the $\frac{1}{2}^-$ ^{15}N core; this transition is therefore expected to be essentially pure $L=2$.

From Fig. 6 we see that only fits with Sets I and II are acceptable for the $L=0$, 3.053-MeV transition; and that neither of these give very good fits for the 3.845-MeV, $L=2$ transition. While this may be indicative of more serious problems with the DWBA method of analysis or the optical-model wave functions used, we have extended our search for optical parameters to find a set which would give acceptable fits for both $L=0$ and $L=2$ transitions.

In their reanalysis of the data of Artemov *et al.*[37]

TABLE III. Optical-model parameters for ^{3}He and protons. Sets I through V of ^{3}He parameters were obtained by fitting our elastic scattering data. Sets II and VI were actually used in DWBA analysis of reaction data:

$$V(r) = V_C(r, r_C) - V_0 \frac{1}{e^x+1} - i\left(W_i - 4W_{Di}\frac{d}{dx_i}\right)\frac{1}{e^{x_i}+1} - V_S \frac{\hbar}{m_\pi c^2}\frac{1}{r}\frac{d}{dr}\frac{1}{e^x+1}\vec{l}\cdot\vec{s},$$

where $x=(r-r_0)/a_0$, $x_i=(r-r_i)/a_i$.

Set	V_0 (MeV)	r_0 (F)	a_0 (F)	W_{Di} (MeV)	W_i (MeV)	r_i (F)	a_i (F)	r_C (F)	V_{SO} (MeV)	χ^2
					^{3}He potentials					
I	273.14	1.137	0.692		16.69	1.541	0.924	1.25		2.27
II	177.29	1.194	0.640		12.59	1.671	0.936	1.25		1.97
III	158.36	1.301	0.592		16.58	1.382	1.080	1.25		2.21
IV	103.01	1.272	0.649		8.89	1.863	0.929	1.25		2.04
V	50.10	1.355	0.659		5.36	2.178	0.835	1.25		2.64
VI	200.00	1.250	0.633		10.40	1.930	0.837	1.25		···
					p potential					
	42.64	1.250	0.650	8.04	···	1.250	0.470	1.25	8.5	···

on the scattering of 16.6- and 25.8-MeV ^{3}He by ^{16}O, Mangelson, Harvey, and Glendenning[38] have obtained two sets of parameters. Of these two, the set for 25.8-MeV scattering has almost the same geometry ($V_0r_0^2 = 365$ MeV fm^2) as that obtained by Bohne *et al.*[39] ($V_0r_0^2 = 290$ MeV fm^2) in their analysis of 11-MeV ^{3}He scattering by ^{15}N. We have therefore also used a set of ^{3}He optical-model parameters with a geometry the same as that of Mangelson, Harvey, and Glendenning[38] (but with $V_0 = 200$ MeV, $V_0r_0^2 = 312$ MeV fm^2 in order to adapt to our lower energy). It is found that this set (labeled VI in Table III) gives an $L = 0$ fit which is somewhat better than that of Set II, and that the $L = 2$ fit shows definite improvement (see Figs. 10 and 12). On the other hand, it must be pointed out that this set of optical-model parameters gives totally unacceptable fits to our elastic scattering data, as is also indicated in Fig. 5. These problems indicate that a systematic study of ^{3}He scattering from ^{15}N in the energy range 10 to 30 MeV would be very desirable. An excitation-function study may also give valuable information.

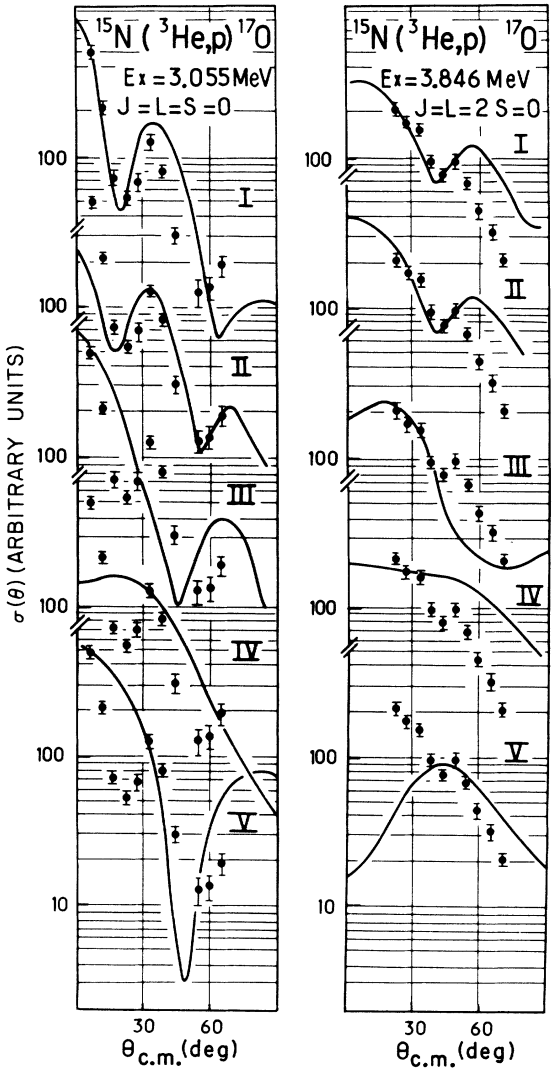

FIG. 6. DWBA fits to (^{3}He,p) differential cross sections for the $L = J = 0$ transition to the 3.053-MeV ($\frac{1}{2}^-$) state and for the $L = J = 2$ transition to the 3.845-MeV ($\frac{5}{2}^-$) state using different sets of ^{3}He optical-potential parameters in Table III. Notice that Set II provides the best over-all fits to both $L = 0$ and $L = 2$ transitions. For fits corresponding to Set VI see Figs. 10 and 12.

In the DWBA analyses reported in this paper we have used ^{3}He parameters of both Set II and those based on Mangelson's geometry – Set VI. As mentioned before, the proton parameters are those based on Perey's[36] systematics, except for the addition of a 8.5-MeV $\vec{l}\cdot\vec{s}$ potential which is found to improve fits in the minima of $L = 0$ transitions.

5. DWBA ANALYSIS OF REACTION DATA

Formalism

It is not our purpose here to go into details of the DWBA analysis of two-nucleon-transfer reactions. These have been described in detail by Glendenning,[40] whose formalism we employ here. However, it is necessary to review the method briefly in order to bring out the essential feature of these reactions.

Consider the transition between the *initial* state ($J_i\pi_iT_i$) of the target nucleus ($A-2$) and the *final* state ($J_f\pi_fT_f$) of the residual nucleus A. Let the reduced mass of the light "particle" and the wave number in the incident channel be given by μ_i and $\vec{k}_i$, and those in the outgoing channel by μ_f and $\vec{k}_f$. Let the quantum numbers of the two transferred particles be labeled by subscripts 1 and 2 on lower case letters and those of the pair by capital letters. Then

$$\vec{L} = \vec{l}_1 + \vec{l}_2\,; \quad \vec{S} = \vec{s}_1 + \vec{s}_2\,; \quad \vec{J} + \vec{L} + \vec{S} = \vec{j}_1 + \vec{j}_2\,,$$
$$\vec{J}_f = \vec{J} + \vec{J}_i\,; \quad T_f = \vec{T} + \vec{T}_i\,; \quad \pi_i\pi_f = (-1)^L\,. \qquad (1)$$

The angular distribution for a two-nucleon-transfer reaction is characterized by the transferred angular momentum, much the same as for a single-nucleon-transfer reaction. However, since in this case the total angular momentum L is carried by two nucleons, many different configurations for the two individual nucleons ($n_1l_1j_1, n_2l_2j_2$, collectively denoted by script γ) can contribute. These contributions give rise to coherence and therefore the two-nucleon-transfer *cross sections* cannot be factorized into a part containing the kinematic information of the reaction and another containing the nuclear-structure information, as is possible in single-nucleon-transfer reactions:

$$\frac{d\sigma(\theta)}{d\Omega}=\frac{2J_f+1}{2J_i+1}\sum_{LJST} D^2(S)C_{ST}{}^2\,\sigma_{LJST}(\theta),$$

$$\sigma_{LJST}(\theta)=\sum_{M_L}\sum_{N}|G_{NLJST}B^{M_L}_{NL}(\vec{k}_i,\vec{k}_f)|^2\frac{\mu_i\mu_f}{(2\pi\hbar^2)^2}\frac{k_f}{k_i}, \tag{2}$$

where $D(S)$ is the zero-range interaction strength between the nucleons in ^{3}He, and $C_{ST}{}^2$ are coefficients describing spin and isospin coupling. In this expression all the nuclear-structure information is contained in the G_{NLSJT} which in turn are sums over the many configurations $\gamma(n_1l_1j_1,n_2l_2j_2)_{NLJ}$. The $B^{M_L}_{NL}$ contain only the kinematic information of the reaction. They are amplitudes for transfer of a structureless pair of nucleons, the motion of whose center of mass is characterized by quantum numbers N, L, M_L and radial wave functions $U_{NL}(R)$.

S	T	T_f-T_i	$J(j^2)$
1	0	0	odd
0	1	0 ($T_i\neq0$)	even
0	1	1	even

$J(j_1j_2)$	$C_{ST}{}^2$
	$\frac{1}{2}$
$J+\Delta\pi$ even	$T_i[2(T_i+1)]^{-1}$
$J+\Delta\pi$ even	$(2T_i+1)[2(T_i+1)(2T_i+3)]^{-1}$

Since ^{15}N(g.s.) has $J^\pi_i=\frac{1}{2}^-$, $T_i=\frac{1}{2}$, for the $T_f=\frac{1}{2}$ states populated in the reaction ^{15}N(^{3}He, p)^{17}O; in general, at least two T values, two J values, and two L values contribute. The lower permissible L transfer, however, tends to dominate the shape of the angular distribution.

In general, the interaction $D(S)$ between the outgoing proton and each of the particles of the transferred pair in ^{3}He may be S-dependent. We may, therefore, write

$$D(S=0)\equiv D_0$$

and

$$R(S)\equiv|D(S)/D_0|^2.$$

In terms of the cross sections calculated by the code JULIE

$$\sigma^{\rm JULIE}_{LJST}(\theta)=0.509\times10^4\sigma_{LJST}(\theta),$$

$$\frac{d\sigma(\theta)}{d\Omega}=\mathfrak{N}\frac{2J_f+1}{2J_i+1}\sum_{LJST}R(S)C_{ST}{}^2\sigma^{\rm JULIE}_{LJST}(\theta),$$

where the over-all normalization constant

$$\mathfrak{N}=D_0{}^2/(0.509\times10^4),$$

where $D_0{}^2$ is in units of MeV^2 fm^3. In practice $\mathfrak{N}$ is empirically determined and includes in it the cumulative effect of the many simplifying assumptions and approximations made in the DWBA analysis of the data, as well as in the model wave functions used in these calculations.

The integrals $B^{M_L}_{NL}$ are actually identical to those which occur in single-particle stripping, except in one aspect. In single-nucleon stripping only one principal quantum number n is involved; in two-nucleon stripping many N values are generally possible. Codes written for DWBA calculations of single-nucleon stripping can, therefore, be very simply adapted to two-nucleon stripping by substituting the two-nucleon "form factor" $\sum_N G_{NLJST}U_{NL}(R)$ for the single-nucleon form factor $u_{nl}(r)$ in the integrals B, which are in both cases evaluated with distorted waves in both the entrance and exit channels. In the calculations reported in this paper we have used the DWBA code JULIE of Bassel, Drisko, and Satchler[41] with the two-nucleon "form factors" calculated by the code FFG due to Laget.[42]

For the (^{3}He, p) reaction the following selection rules hold:

Effects of Variation of Parameters

We have already commented on the effect of the choice of optical-potential parameters on (^{3}He, p) angular distributions. Having made the choice of these parameters, it is possible to investigate the effect of several other parameters which enter into the analysis of the observed angular distributions. We discuss some of these results below.

The single-particle wave functions used were calculated in a harmonic-oscillator potential with oscillator energy $\hbar\omega=41A^{-1/3}$, or the oscillator parameter $\nu=0.40$ fm^2 (defined with ν so that the single-nucleon wave functions are proportional to $e^{-(1/2)\nu r^2}$). It was found that the effect of varying ν (within ±10% of this value) was to alter the relative heights of the first and second maxima, and that $\nu=0.40$ fm^{-2} was optimum.

For numerical calculation of angular distributions, in the asymptotic region the harmonic-oscillator wave function is replaced by the Hankel function $-i^Lh_L(ikr)$, where k is the wave number corresponding to the binding energy ϵ of the transferred pair in the residual nucleus. We have used the usual well-depth convention for the binding energy; i.e., $\epsilon=B(n,p)+E_x$, where $B(n,p)$ is the binding energy of the last proton and neutron in the ground state of the residual nucleus and E_x is the excitation energy for the level in question. One can, however, use any one of the several other alternatives which have been suggested. We have investigated the effect of changing ϵ on $J=L=0$ transitions and

find that a 2-MeV decrease in ϵ may increase the cross sections by up to 10% and may produce as much as a 5° phase shift in the structure of the angular distributions. The effect is most pronounced for levels at high excitation and almost negligible for low-lying levels.

The size parameters η for ^{3}He can be deduced from the relation $\eta^2 = 1/(6\langle r^2\rangle)$. Using $\langle r^2\rangle^{1/2} = 1.97$ fm from electron scattering experiments, we get $\eta = 0.206$ fm^{-1}. It was found that cross sections were rather insensitive to reasonable variations of η around this value.

As an example of the degree of sensitivity that (^{3}He, p) angular distributions possess to the mixing of configurations, we have calculated the angular distribution for the 3.053-MeV state in ^{17}O under three different assumptions: (a) The transferred pair is entirely in the configuration $(d_{5/2})^2_{L=J=T=0}$; (b) the transferred pair is entirely in the configuration $(s_{1/2})^2_{L=J=T=0}$; and (c) the transferred pair is in the mixed configuration $-0.3(s_{1/2})^2 - 0.63(d_{5/2})^2$. The shape of the angular distribution in each case is found to be the same, namely, that in Fig. 10, but the absolute cross sections are found to differ considerably as follows:

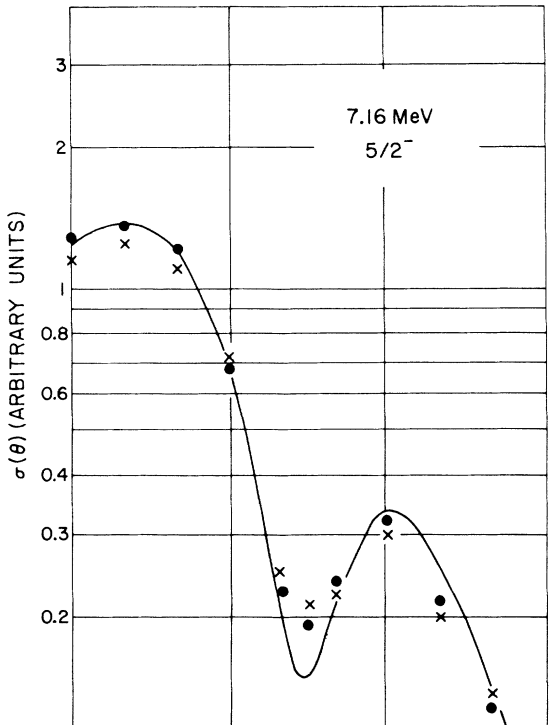

FIG. 7. Illustration of the effect of interference between contributions due to $S=0$ and $S=1$ terms for the $J=L=2$ transition to the 7.162-MeV $\frac{5}{2}^-$ state. The solid line corresponds to $V_{so}=0$, i.e., the case when the two terms contribute incoherently. Crosses and filled circles correspond to a calculation with $V_{so}=8.5$ MeV: crosses, when the interference term is included; and filled circles, when the interference term is neglected.

$$\text{Config.}: (d_{5/2})^2 : (s_{1/2})^2 : [-0.3(s_{1/2})^2 - 0.63(d_{5/2})^2]$$

$$d\sigma/d\Omega : \quad 1 \quad : \quad 4 \quad : \qquad 0.7 .$$

As mentioned in Sec. 4 the proton optical potential used has a spin-orbit term. In the presence of this term Eq. (2) is not correct, since the following terms contribute coherently:
(a) for $J \geq 1$, $L = J-1$ and $J+1$;
(b) for $L = J$, $S = 0$ and 1.
Laget[42] has shown that the interference term due to (a) makes a negligible contribution. We have verified this to be true in our case also. We have further determined that interference due to (b) is also negligible. This is illustrated in Fig. 7 for the 7.162-MeV transition for which $J_f = \frac{5}{2}^-$ and $J = L = 2$, and $S = 0$ or 1 are both possible. The calculations reported in this paper were therefore all done without interference terms due to (a) or (b).

Qualitative Features of Differential Cross Sections

In Fig. 8 we show a plot of relative intensities of levels as observed in the 15° spectrum. Such plots are often used to illustrate preferential excitation of certain states. However, at least in our case, such a conclusion is apt to be very misleading. The reasons for this are clear from Fig. 8. In Fig. 8 we have plotted the cross sections, integrated between 5 and 65° and divided by $(2J+1)$, for most of the transitions for which the observed angular distributions were complete or for which relatively convincing interpolations and extrapolations could be made for the one or two angles at which cross sections could not be measured. It is seen in Fig. 8 that the reduced cross sections are remarkably constant, the extreme variation being less than a factor 2 for levels of one-parity character. The same observation was made earlier by Seth *et al.*[1,2] In the present data there appears to be some tendency for gradually weaker excitation of positive-parity states as one goes to higher excitation energies. This trend indicates that the positive-parity states are indeed excited mainly through their 1p-0h components. The correlated 2p-3h part of ^{15}N(g.s.) does not play a significant role, and we can essentially neglect it and take account of the neglect by "renormalizing" the corresponding ^{17}O wave functions. This is, indeed, what was done in

order to calculate theoretical cross sections.

The 4p-3h components of negative-parity states of ^{17}O are only poorly accessible to the reaction ^{15}N(^{3}He, p)^{17}O. They should, however, be most accessible to the reaction ^{13}C(^{7}Li, t)^{17}O. Indeed, in this reaction it is found that the low-lying negative-parity states (those at 3.053, 3.845, and 4.549 MeV) are strongly excited.[31,32] The relatively weaker excitation of these states in our experiment and their strong excitation in the reaction ^{13}C-(^{7}Li, t)^{17}O together confirm the prediction of most of the recent theoretical calculations that these states have predominantly 4p-3h components (see Table I). In the phenomenological description of Brown and Green[14] this would correspond to a confirmation of the conjecture that the 4p-4h deformed state of the ^{16}O core lies lower than the 2p-2h deformed state.

We may also compare our results qualitatively with those of the (α, d) experiment of LZH[7]. We make this comparison in terms of σ(total)/$(2J+1)$ In our experiment (see Fig. 8) the reduced total cross sections for the $\frac{5}{2}^+$ ground state and the $\frac{1}{2}^+$ (0.874-MeV) state are nearly equal. LZH find the cross section for the $\frac{1}{2}^+$ state to be $\frac{1}{3}$ of that for the $\frac{5}{2}^+$ ground state. While this may in part be due to the fact that in their experiment at $E_\alpha = 45.4$ MeV high-angular-momentum transfer should be emphasized, this difference arises largely from their having missed the first maximum of the predominantly $L=1$ transfer. For the same reason their reduced cross section for the 4.549-MeV ($L=0$) transition is quoted as only 70% of that for the 3.845-MeV ($L=2$) transition, whereas in our experiment the two have equal strength. A more significant comparison is that for the $L=4$ transitions to the $(d_{5/2}{}^2 p_{1/2}{}^{-1})$ states of spins $\frac{11}{2}^-$ (7.761 MeV) and $\frac{9}{2}^-$ (9.16 MeV). LZH find these reduced

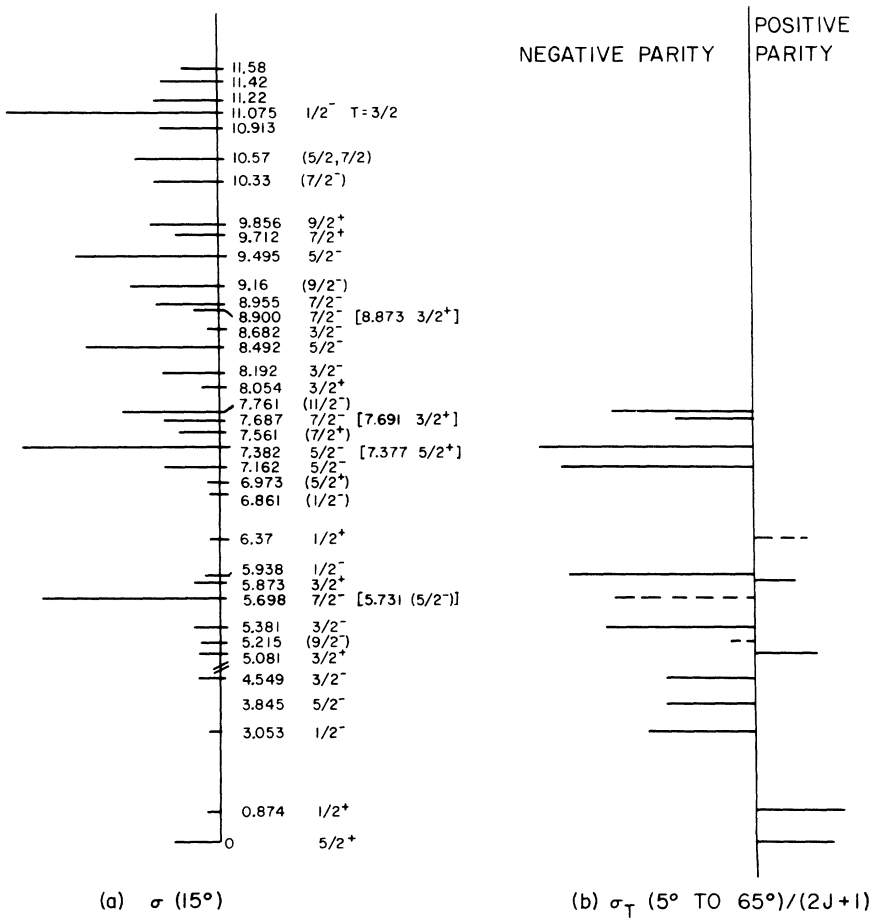

FIG. 8. Schematic representation of relative cross sections for transitions to the different states in ^{17}O: (a) differential cross section at $\theta_{lab} = 15°$, (b) integrated cross sections ($\theta = 5$ to 65°) divided by $(2J_f+1)$. The dashed lines corresponds to the cases where J_f is uncertain or where a multiplet of levels of the same parity are involved. In that case $\sum(2J_f+1)$ is used as divisor. When a positive-parity level is unresolved from a negative-parity level, the positive-parity-level contribution has been neglected.

cross sections to be in the ratio of 2:1; whereas, if we neglect the contribution due the unresolved $L=0$ transition to the $\frac{1}{2}^-$ state at 9.14 MeV (i.e., neglect cross sections below $\theta=15°$), our reduced cross sections for the two states are equal, which is what is to be expected if the proposed explanation for the structure of these states is correct. Undoubtedly, the reason for this discrepancy lies in the inability of LZH to resolve the 7.761-MeV transition from the 7.561- and 7.687-MeV transitions, which together have an almost equal integrated cross section in our experiment. The absence of the 11.075-MeV transition in the (α, d) experiment is a confirmation of the $T=\frac{3}{2}$ nature of this state which is populated strongly in our $(^3\mathrm{He}, p)$ experiment.

Angular Distributions

As mentioned earlier, in order to do a detailed analysis of the observed angular distributions, we require model wave functions for states in ^{17}O and for the ground state of ^{15}N. For this purpose we have chosen the wave functions given by ZBM. These wave functions are listed in Tables IV and V, where the correspondence of the experimental states with the most likely states of the ZBM calculation is also indicated. This correspondence is also shown in Fig. 9, where the slightly modified predictions of the optimized calculation due to WM are also shown. As mentioned in Sec. 2, in most cases there are no problems in establishing the correspondence up to an excitation of 6.5 MeV. Below this energy the only problematic cases are the 5.215-MeV state and the 5.731-MeV state for which definite spin assignments are not available, and the 5.081-MeV state which is mainly $d_{3/2}$ single particle in nature. Since in the ZBM calculation the $d_{3/2}$ orbit is not considered active, there is no corresponding state in their results. On circumstantial evidence alone there is a great temptation to identify the 5.215-MeV state with the 4.79-MeV $\frac{9}{2}^-$ state of ZBM, and the 5.731-MeV state with the 5.85-MeV $\frac{5}{2}^-$ state of ZBM. We shall return to these cases later.

Above 6.5 MeV we can establish correspondence only in a few cases with certainty. A large number of states predicted by ZBM can, however, be iden-

TABLE IV. ^{17}O wave functions according to Zuker, Buck, and McGrory: negative-parity states. Only amplitudes larger than 0.2 have been retained.

J^π	E(exp) (MeV)	E(theor) (MeV)	2p-1h components [(2p amplitudes)$\otimes p^{-1}(\frac{1}{2}\frac{1}{2})]_{J,1/2}$	4p-3h components [a] [(4p amplitudes)$\otimes p^{-3}(\frac{1}{2}\frac{1}{2})]_{J,1/2}$
$\frac{1}{2}^-$	3.053	2.88	$-0.57d^2(01)-0.27s^2(01)$	$+0.34[d^2s^2](00)-0.43d^4(00)$
$\frac{1}{2}^-$	5.958	5.74	$+0.21d^2(01)-0.51d^2(10)-0.57s^2(10)$	$-0.29[d^2s^2](11)$
$\frac{1}{2}^-$	6.861	6.77	$+0.68d^2(01)-0.36s^2(01)+0.27s^2(10)$	$+0.23[d^2s^2](00)+0.25[d^2s^2](01)$
$\frac{1}{2}^-$	7.938	8.54	$+0.29d^2(10)+0.67s^2(01)$	$-0.36[d^2s^2](01)$
$\frac{3}{2}^-$	4.549	4.51	$-0.38d^2(10)+0.50d^2(21)-0.40s^2(10)+0.26[ds](21)$	$+0.27[d^3s](20)+0.31d^4(20)$
$\frac{3}{2}^-$	5.381	5.41	$+0.38d^2(10)+0.47s^2(10)+0.37[ds](21)$	$+0.37[d^3s](20)$
$\frac{3}{2}^-$	7.67	(7.16)	$-0.65d^2(21)-0.35s^2(10)+0.24[ds](21)$	$+0.22[d^3s](20)-0.33d^4(21)$
$\frac{3}{2}^-$	8.192	(8.49)	$-0.55[ds](20)+0.47[ds](21)$	$-0.42[d^3s](21)$
$\frac{5}{2}^-$	3.845	3.48	$+0.62d^2(21)+0.39[ds](21)$	$+0.30[d^3s](20)+0.32d^4(20)$
$\frac{5}{2}^-$	5.731	5.85	$-0.53d^2(21)+0.49[ds](21)$	$+0.34[d^3s](20)-0.27d^4(21)$
$\frac{5}{2}^-$	7.382	6.78	$-0.47d^2(30)-0.66[ds](30)$	$-0.22[d^3s](31)-0.21d^4(31)$
$\frac{5}{2}^-$	7.162	7.97	$+0.54[ds](20)+0.36[ds](21)$	$+0.32[d^3s](21)$
$\frac{7}{2}^-$	5.698	5.69	$+0.49d^2(30)+0.65[ds](30)+0.25[ds](31)$	$+0.26[d^3s](31)+0.23d^4(31)$
$\frac{7}{2}^-$	7.687	8.01	$-0.72d^2(41)-0.32[ds](30)$	$-0.27d^4(401)+0.31d^4(411)$
$\frac{9}{2}^-$	5.215	(4.79)	$-0.31d^2(50)+0.78d^2(41)$	$+0.27d^4(40)$
$\frac{9}{2}^-$	9.16	7.09	$-0.83d^2(50)-0.30d^2(41)$	$+0.37d^4(51)$
$\frac{11}{2}^-$	7.761	6.00	$+0.89d^2(50)$	$-0.41d^4(51)$

[a] Only those 4p-3h components, which have $d^2(01)$, and therefore finite overlap with ^{15}N(g.s.) 2p-3h component, $d^2(01)$, are listed. $^{15}\mathrm{N(g.s.)}=0.88p^{-1}+0.44d^2(01)p^{-3}$.

TABLE V. ^{17}O wave functions according to Zuker, Buck, and McGrory: positive-parity states. Only amplitudes larger than 0.2 have been retained.

J^π	E(exp) (MeV)	E(theor) (MeV)	1p-0h	3p-2h [a] [(3p amplitudes)$\otimes p^{-2}(01)]_{J,1/2}$	3p-2h [(3p amplitudes)$\otimes p^{-2}(10)]_{J,1/2}$
$\frac{1}{2}^+$	0.874	0.83	$+0.78s$	$+0.34[d^2s](\frac{1}{2}\frac{1}{2})+0.39[d^2s](\frac{1}{2}\frac{3}{2})$	
$\frac{1}{2}^+$	6.37	6.76	$-0.27s$		$-0.40[d^2s](\frac{1}{2}\frac{1}{2})$
$\frac{3}{2}^+$	5.081	...	...	No corresponding state	...
$\frac{3}{2}^+$	5.867	5.28	...	0	0
$\frac{3}{2}^+$	7.294	7.01			$+0.39[d^2s](\frac{1}{2}\frac{1}{2})$
$\frac{3}{2}^+$	8.054	(7.56)			$+0.30[d^2s](\frac{1}{2}\frac{1}{2})$
$\frac{3}{2}^+$	8.873	(8.65)			$-0.46d^3(\frac{5}{2}\frac{1}{2})$
$\frac{5}{2}^+$	0.0	0.0	$+0.82d$	$-0.32d^3(\frac{5}{2}\frac{1}{2})+0.37d^3(\frac{5}{2}\frac{3}{2})$	
	6.973	6.81	$+0.27d$	$-0.23d^3(\frac{5}{2}\frac{3}{2})$	$+0.30d^3(\frac{5}{2}\frac{1}{2})$
	7.377	7.66	$-0.27d$	$-0.29d^3(\frac{5}{2}\frac{1}{2})$	$-0.36d^3(\frac{5}{2}\frac{1}{2})$
$\frac{7}{2}^+$	7.561	(7.24)			$-0.62d^3(\frac{5}{2}\frac{1}{2})$

[a] Only those 3p-2h components which have $d^2(01)$, and therefore finite overlap with the ^{15}N(g.s.) 2p-3h component, $d^2(01)$, are listed. ^{15}N(g.s.) is $0.88p^{-1}+0.44d^2(01)\,p^{-3}$.

TABLE VI. Relative normalization constants (referred to those required for the transitions to the states at 5.698 and 5.731 MeV) for various approximations used in DWBA analyses.

No.	E^* (MeV)	J^π	$\mathfrak{N}(E^*)/\mathfrak{N}$(5.7 MeV) Set-II ^{3}He potential [a] $R(S)=1.0$	Set-II ^{3}He potential [a] $R(S)=0.5$	Set-VI ^{3}He potential [b] $R(S)=1.0$	Set-VI ^{3}He potential [b] $R(S)=0.5$
0	0	$\frac{5}{2}^+$	1.5	1.4	1.1	1.0
1	0.874	$\frac{1}{2}^+$	0.5	0.5	...	...
2	3.053	$\frac{1}{2}^-$	2.0	1.0	2.5	1.25
3	3.845	$\frac{5}{2}^-$	2.8	1.4	2.5	1.25
4	4.549	$\frac{3}{2}^-$	0.85	0.8	0.5	0.5
6	5.215	$(\frac{9}{2}^-)$	1.7	1.4	0.65	0.62
7	5.381	$\frac{3}{2}^-$	0.8	0.8	1.0	1.0
8	5.698	$\frac{7}{2}^-$	1.0	1.0	1.0	1.0
9	5.731	$(\frac{5}{2}^-)$				
11	5.938	$\frac{1}{2}^-$	1.3	1.3	1.0	1.0
13	6.861	$\frac{1}{2}^-$	3.0	2.8	2.4	2.5
14	6.973	$(\frac{5}{2}^+)$	3.2	3	2.4	2.1
15	7.162	$\frac{5}{2}^-$	1.7	1.4	0.9	0.7
17	7.377	$\frac{5}{2}^+$	1.15	1.2	1.15	1.1
18	7.382	$\frac{5}{2}^-$				
21	7.687	$\frac{7}{2}^-$	1.8	1.6	1.05	1.05
23	7.761	$(\frac{11}{2}^-)$	1.8	1.5	1.7	1.6
36	9.16	$(\frac{9}{2}^-)$	1.7	1.8	1.4	1.1

[a] $\mathfrak{N}$(5.7 MeV) = 9.3 × 3.74 = 34.8.

[b] $\mathfrak{N}$(5.7 MeV) = 14.4 × 3.74 = 53.9.

tified with experimental states with reasonable confidence on the basis of excitation energy and J^{π}, as indicated in Fig. 9. The insensitivity of the excitation-energy predictions to variation of the parameters of the calculation, as evidenced from a comparison of the ZBM results with WM results, determines to an extent the degree of confidence with which such correspondence can be made. For example, the J^{π} are not known for states at 6.861, 6.973, and 7.561 MeV. The unassigned states in the calculations, in the vicinity of these excitation energies, are the 6.77-MeV ($\frac{1}{2}^-$), 6.88-MeV ($\frac{5}{2}^+$), and the 7.24-MeV ($\frac{7}{2}^+$) states in the ZBM calculation and the corresponding 5.81-MeV ($\frac{5}{2}^+$), 6.77-MeV ($\frac{7}{2}^+$), and 7.53-MeV ($\frac{1}{2}^-$) states in the WM calculation. Since the ordering of these states is completely different in the two cases, we cannot make any reliable correspondence. We shall have to look into other evidence.

According to ZBM, the ground-state wave function of ^{15}N is mainly

$$0.88p_{3/2}{}^{-1}+0.44d^2(01)p_{3/2}{}^{-3}.$$

In the (^{3}He, p) reaction, the negative-parity states populated in ^{17}O can have a 2p-1h or 4p-3h nature, and the positive-parity states can have a 1p-0h or 3p-2h nature. In our DWBA calculations, we have neglected the explicit consideration of the correlated part of the ^{15}N(g.s.) wave function (for *a posteriori* justification see Sec. 6). This simplifies DWBA calculations but limits us to negative-parity states with finite 2p-1h components and positive-parity states with finite 1p-0h components. Contributions of 3p-2h components in wave functions were included only in the sense that the weak-coupling picture of the final states seems to hold for sever-

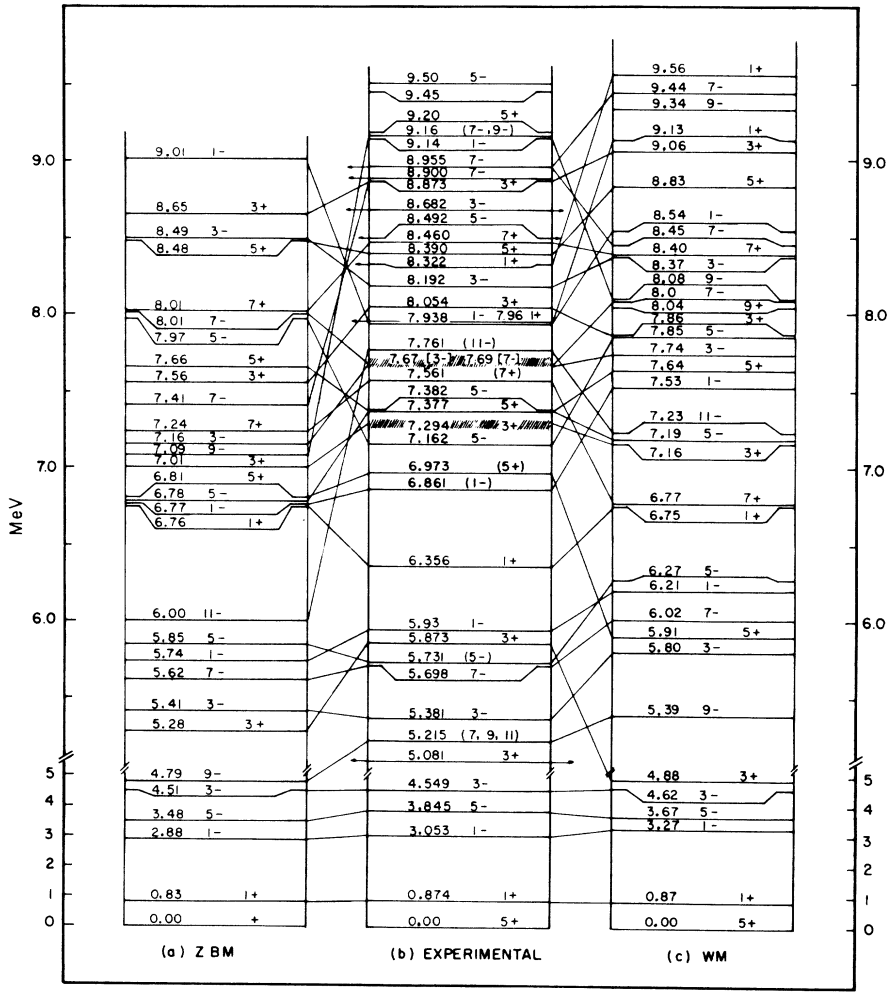

FIG. 9. The spectrum of states in ^{17}O; E and $2J^{\pi}$ are shown: (a) results of calculations of Zuker, Buck, and McGrory (Ref. 20); (b) experimental; and (c) results of calculations of Wildenthal and McGrory (Ref. 21).

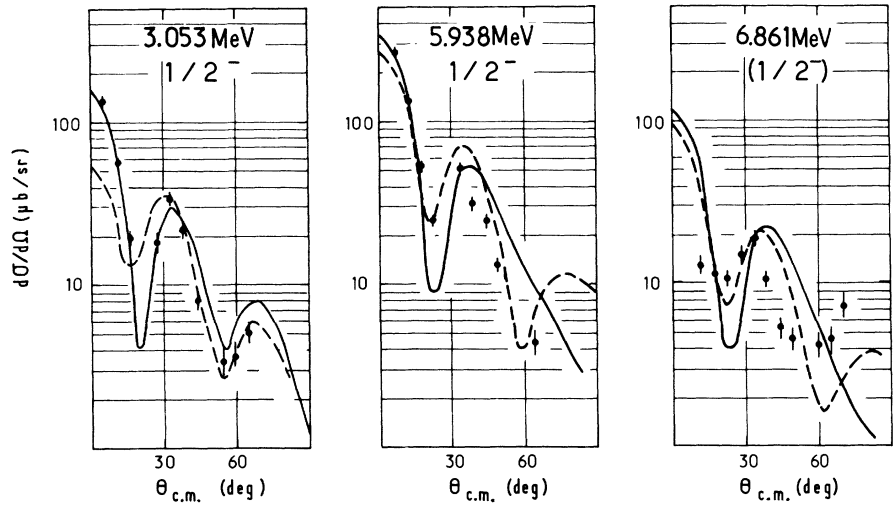

FIG. 10. Measured differential cross sections for $\frac{1}{2}^-$ states and the $L=0$ DWBA fits to them using wave functions due to ZBM. Solid curves correspond to ^{3}He parameters of Set VI. Dashed curves correspond to ^{3}He parameters of Set II.

al states in ^{17}O (see Sec. 6). Figures 10 through 14 display the fits to experimental data obtained by using ZBM wave functions for those cases in which correspondence between experimental states and those predicted by ZBM could be made. In each case the curves indicate DWBA fits to the data – solid lines, using the Set-VI ^{3}He potential, and dashed lines, using the Set-II ^{3}He potential. The normalization used for the theoretical curves is discussed below.

If we normalize the theoretical DWBA curves to the experimental cross sections, we determine the normalization constant $\mathfrak{N}$. For the unresolved transition corresponding to the levels at 5.698 MeV ($\frac{7}{2}^-$) and 5.731 MeV ($\frac{5}{2}^-$), the empirical value of $\mathfrak{N}$ is found to be

$$\mathfrak{N}_{\text{exp}} = 35, \text{ for Set-II } ^3\text{He parameters}$$
$$= 54, \text{ for Set-VI } ^3\text{He parameters}.$$

These values are to be contrasted with

$$\mathfrak{N}_{\text{theor}} = 3.74,$$

which is obtained if a Gaussian wave function is assumed for ^{3}He.

Fits to other transitions lead to values of the normalization constant $\mathfrak{N}$ which do not differ from the above by a factor greater than 2 in most cases. In Table VI we summarize our results for the ra-

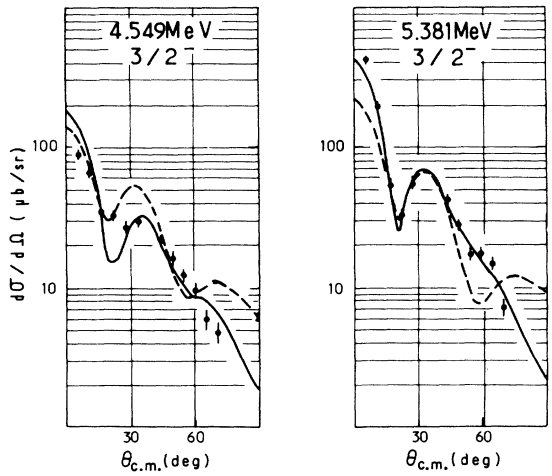

FIG. 11. Measured differential cross sections for $\frac{3}{2}^-$ states and the $L=0$ DWBA fits to them using wave functions due to ZBM. Solid curves correspond to ^{3}He parameters of Set VI. Dashed curves correspond to ^{3}He parameters of Set II.

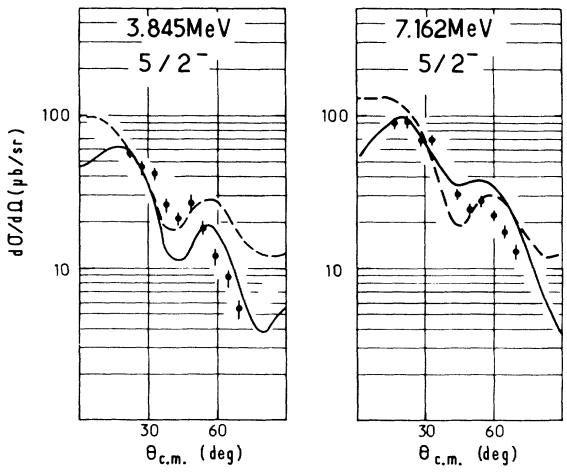

FIG. 12. Measured differential cross sections for $\frac{5}{2}^-$ states and the $L=2$ DWBA fits to them using wave functions due to ZBM. Solid curves correspond to ^{3}He parameters of Set VI. Dashed curves correspond to ^{3}He parameters of Set II.

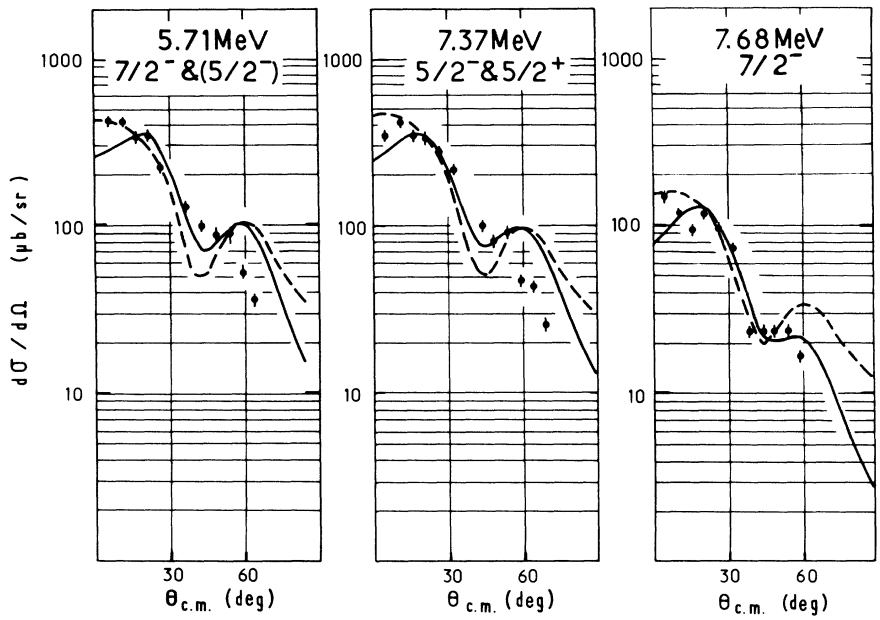

FIG. 13. Measured differential cross sections for 5.71-, 7.37-MeV states and the $L=2$ DWBA fits to them using wave functions due to ZBM. The fits shown for the 7.687-MeV transition are $L=2$. The $\frac{3}{2}^-$ state is 400 keV wide and makes no identifiable contribution above background. Solid curves correspond to ^{3}He parameters of Set VI. Dashed curves correspond to ^{3}He parameters of Set II.

tio $\mathfrak{N}(E^*)/\mathfrak{N}(5.7\ \text{MeV})$. The numbers listed were obtained by fitting the data with the theoretical curves based on the Set-II ^{3}He potential as well as those based on the Set-VI ^{3}He potential. It is seen that no preference for either set is indicated; the ratio shows approximately the same range of variation in both cases. For each set fits were obtained for both $R(S)=1.0$ and 0.5; once again the normalization constants so determined do not indicate any clear-cut preference for either value of $R(S)$. This is not surprising, since most transitions have both $S=0$ and $S=1$ components, and the effect of choosing different values of $R(S)$ is mostly absorbed in the absolute value of the normalization constant $\mathfrak{N}$.

It is difficult to comment on the implications of the departure of $\mathfrak{N}\ (E^*)/\mathfrak{N}(5.7\ \text{MeV})$ from unity. Fits to the data are far from being excellent, espe-

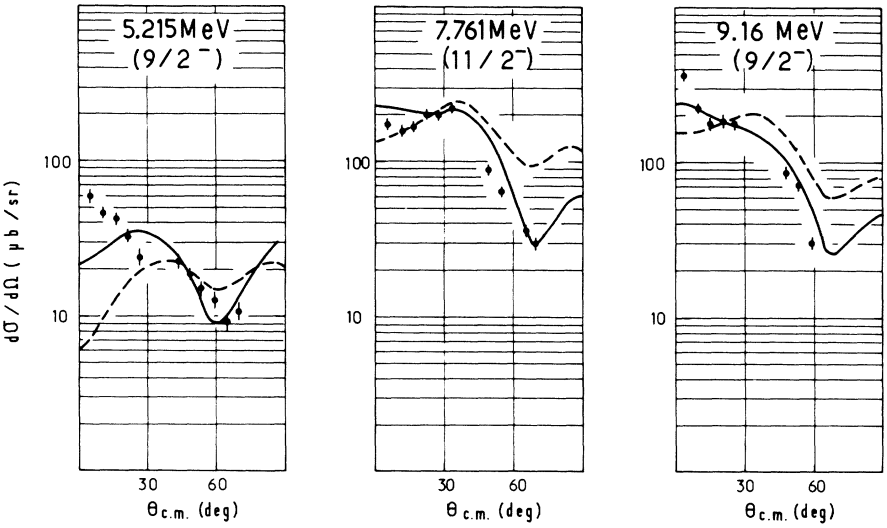

FIG. 14. Measured differential cross sections for 5.215-, 7.761-, and 9.16-MeV states and the $L=4$ DWBA fits to them using wave functions due to ZBM. Solid curves correspond to ^{3}He parameters of Set VI. Dashed curves correspond to ^{3}He parameters of Set II.

cially for $L \neq 0$. Also the model wave functions have only been used in an approximate and simplified manner (e.g., the correlated part of the target wave function was neglected) and this tends to introduce large errors in weak transitions, as for example in the case of weak 3.053-, 3.845-, 6.861-, and 6.973-MeV transitions.

The characteristic of predominantly $L=0$ angular distributions is their first maximum at 0° with as much as a factor of 10 decrease in the cross section by about 20°. A glance at Figs. 10 and 11 shows that transitions to the $\frac{1}{2}^-$ states at 3.053 and 5.938 MeV and to the $\frac{3}{2}^-$ states at 4.549, 5.381, and 8.192 MeV (Fig. 3) clearly show this behavior. The maximum at $\theta = 30°$ for the 6.861-MeV transition seems to indicate an $L=0$ transition. However, if this is true the 10° datum point must certainly be in error. The transition to the 8.054-MeV state appears to possess an $L=0$ shape, although the state is known to have spin $\frac{3}{2}^+$ (see Fig. 3). However, the data on this transition are sparce and if the 5° datum point was in error the shape could very well be ascribed to $L=1$ transfer.

Characteristic $L=2$ shapes are seen in the angular distributions for the 3.845-MeV ($\frac{5}{2}^-$), 7.162-MeV ($\frac{5}{2}^-$), and 8.492-MeV ($\frac{5}{2}^-$) states (see Fig. 12). The angular distribution corresponding to the state at 5.698-MeV ($\frac{7}{2}^-$) is very similar in shape (see Fig. 13).

As mentioned earlier, comparison with calculated spectrum of ZBM (and WM) indicates that the spin of the 5.731 state could be $\frac{5}{2}^-$. The corresponding ZBM shell-model wave function of this ($\frac{5}{2}^-$) level has only a 10% effect on the total cross-section magnitude of this doublet. The angular distribution for the 7.382-MeV ($\frac{5}{2}^-$) transition has also been fitted with an $L=2$ shape. The unresolved transition to the 7.377-MeV ($\frac{5}{2}^+$) state makes a very small $L=1+3$ contribution.

The only clear-cut example of an $L=4$ angular distribution is provided by the 7.761-MeV transition (see Fig. 14). This is in agreement with the identification of this state by Harvey and his collaborators as the $[(d_{5/2})^2_{J=5} p_{1/2}{}^{-1}]_{11/2^-}$ state. The $\frac{9}{2}^-$ member of this state, as identified by the same authors, would be at 9.16 MeV. This transition is unfortunately not so convincingly identifiable as $L=4$, since it apparently contains a contribution due to the $L=0$ transition to the $\frac{1}{2}^-$ state at 9.14 MeV.

It has been suggested by Rose,[43] on the basis of cross sections for the compound-nuclear reaction $^{14}\mathrm{N}(\alpha, p)^{17}\mathrm{O}$, that the 5.215-MeV state has spin $\frac{7}{2}$, $\frac{9}{2}$, or $\frac{11}{2}$. We have already mentioned that there are theoretical reasons for expecting a $\frac{9}{2}^-$ state in this neighborhood. If we identify the 5.215-MeV state with the 4.79-MeV ($\frac{9}{2}^-$) state of ZBM, we get the angular distribution shown in Fig. 14. The $L=4$ fit is very poor. Actually, the forward peak of the observed angular distribution is more consistent with a predominant $L=2$ or 3 component in this transition. This would, however, limit the maximum spin to $\frac{7}{2}^-$ or $\frac{9}{2}^+$. The reason for this discrepancy is not clear.

Only two transitions to known positive-parity states were analyzed in the present experiment. As shown in Fig. 15 the $L=1$ DWBA fit to the 0.874-MeV ($\frac{1}{2}^+$) state using ZBM wave functions is quite good. On the other hand, the $L=1+3$ DWBA fit to the $\frac{5}{2}^+$ ground state transition is poor. The shape of the experimental angular distribution is closer to that for the pure $L=1$ transition to the 0.874-MeV state than to the theoretical DWBA curve.

As already mentioned, no ZBM wave functions

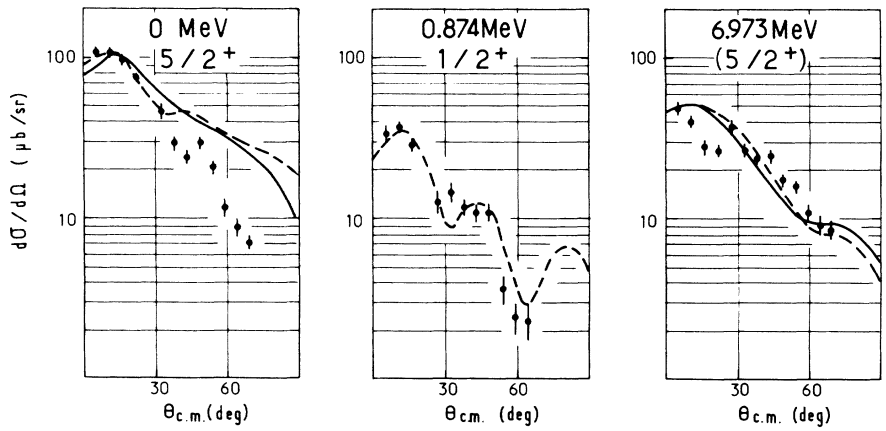

FIG. 15. Measured differential cross sections for the ground state, 0.874-, and 6.973-MeV states and the DWBA fits to them using wave functions due to ZBM. Solid curves correspond to ^{3}He parameters of Set VI. Dashed curves correspond to ^{3}He parameters of Set II.

TABLE VII. ^{17}O states as weak coupling of a $p_{1/2}$ particle or hole to states of ^{16}O and ^{18}F, respectively, according to ZBM (Ref. 20) calculations. In general only amplitudes greater than 0.25 were retained by ZBM. No entry in a column corresponding to a configuration means an amplitude <0.25. In some cases it was possible to find amplitudes for certain configurations from the very similar calculations of Wildenthal and McGrory (Ref. 21). These are quoted in parentheses.

Configuration	Configuration amplitudes		
	^{17}O(3.06 MeV)$\frac{1}{2}^-$		$\|^{16}$O(6.06 MeV)$0^+\rangle\otimes p_{1/2}$
s^4p	−0.28		+0.54
$d^2(01)s^2(01)p$	+0.34		−0.42
$d^2(10)s^2(10)p$	−0.30		+0.43
$d^3(\frac{1}{2}\,\frac{1}{2})sp$	−0.29		+0.33
$d^4(00)p$	−0.43		+0.31
$d^2(01)p^3$	−0.57		...
$s^2(01)p^3$	−0.27		...
	^{17}O(3.85 MeV)$\frac{5}{2}^-$	^{17}O(4.55 MeV)$\frac{3}{2}^-$	$\|^{16}$O(6.92 MeV)$2^+\rangle\otimes p_{1/2}$
$[ds](21)p^3$	+0.39	+0.26	+0.38
$d^2(21)p^3$	+0.62	+0.50	+0.33
$[d^3(\frac{5}{2}\,\frac{1}{2})s](20)p$	+0.30	+0.27	+0.48
$d^4(201)p$	+0.32	+0.31	+0.35
$[ds^3](20)p$	−0.20	−0.20	−0.43
$s^2(10)p^3$	...	−0.40	...
$d^2(10)p^3$	...	−0.38	...
	^{17}O(5.71 MeV)$\frac{7}{2}^-$	^{17}O(7.37 MeV)$\frac{5}{2}^-$	$\|^{18}$F(0.94 MeV)$3^+\rangle\otimes p_{1/2}^{-1}$
$[ds](30)p^3$	+0.65	−0.66	+0.69
$d^2(30)p^3$	+0.49	−0.47	+0.50
$d^4(31)p$	+0.23	−0.21	+0.26
$[ds](31)p^3$	+0.25	(−0.39)	...
$[d^3(\frac{5}{2}\,\frac{1}{2})s](31)p$	+0.26	(−0.19)	+0.21
$[d^3(\frac{5}{2}\,\frac{3}{2})s](31)p$	(+0.17)	(−0.22)	+0.30
$d^2(41)p^3$	−0.23	...	...
	^{17}O(5.38 MeV)$\frac{3}{2}^-$	^{17}O(5.94 MeV)$\frac{1}{2}^-$	$\|^{18}$F(g.s.)$1^+\rangle\otimes p_{1/2}^{-1}$
$s^2(10)p^3$	+0.47	−0.57	+0.65
$d^2(10)p^3$	+0.38	−0.51	+0.51
$[d^2(01)s^2](11)p$		−0.29	+0.39
s^4p		−0.29	...
	^{17}O(7.74 MeV)$\frac{11}{2}^-$	^{17}O(9.16 MeV)$\frac{9}{2}^-$	$\|^{18}$F(1.13 MeV)$5^+\rangle\otimes p_{1/2}^{-1}$
$d^2(50)p^3$	+0.89	−0.83	+0.84
$d^4(51)p$	−0.41	+0.37	−0.46
$d^2(41)p^3$	...	−0.30	...

are available for the 5.081-MeV $\frac{3}{2}^+$ single-particle state; therefore, no DWBA analysis of this transition was made. However, as seen in Fig. 2, it has characteristic $L=1$ shape. This transition could not be analyzed, because, according to the ZBM wave functions, the (^{3}He, p) reaction cannot feed the small 3p-2h components of its wave function (this is indicated by no entry in the corresponding columns in Table V). The state must be populated almost entirely by its 1p-0h component (its 5p-4h components are large, but also inaccessible). Unfortunately, once again, since the $d_{3/2}$ orbit was not considered active in the ZBM calculation, this component is not available either. From Table II, however, we notice that according to Brown and Green the 1p-0h components in the 5.081-MeV ($\frac{3}{2}^+$) and the 5.861-MeV ($\frac{3}{2}^+$) state are 0.72 and 0.26, respectively. Neglecting the higher particle-hole components, which can only be populated via the weaker correlated parts of ^{15}N(g.s.), we expect that the ratio of the measured cross sections for the two transitions should be approximately 2.7/1. This is approximately true, as seen in Figs. 2–4 and 8.

The 7.687-MeV transition (see Fig. 13) is a composite of transitions to the 7.684-MeV ($\frac{7}{2}^-$) and the 7.67-MeV $\frac{3}{2}^-$ state. However, since the 7.67-MeV state is 405 keV wide, its contribution is indistinguishable from background. (In all likelihood some of it has been inadvertently included at the two most forward angles). It is found that ZBM's second $\frac{7}{2}^-$ state at 7.41 MeV cannot account for the observed cross sections of this transition, and correspondence must be made to their third $\frac{7}{2}^-$ state at 8.01 MeV.

6. DISCUSSION AND SUMMARY

The idea of building states of nuclei by weak coupling of a particle or hole to states of adjoining nuclei holds great appeal because of its simplicity. The idea should work particularly well for nuclei near closed shells; the "strong" states of the closed-shell core can be considered as essentially unaltered because of such coupling. Collective states provide excellent candidates for such "strong" core states. We have already seen that the complete microscopic model (ZBM, WM) or the somewhat restricted 2p-1h and 4p-3h calculations of Ellis and Engeland provide a quite good description of negative-parity states of ^{17}O. It is interesting to see how well these same states can be explained as core states of ^{16}O (or ^{18}F) plus a particle (or hole).

Earlier Seth *et al.*[1] attempted to explain several negative-parity states as $s_{1/2}$ and $d_{5/2}$ particles coupled to the strong particle-hole states of the ^{16}O core (3$^-$ at 6.14 MeV, 1$^-$ at 7.12 MeV, and 2$^-$ at 8.88 MeV). Bethge[31] and Schmidt[32] attempted to construct several negative-parity states by coupling a $p_{1/2}$ particle to the 0$^+$ (6.06 MeV), 2$^+$(6.92 MeV), and 4$^+$(10.36 MeV) members of the rotational band in ^{16}O. Ripka[12] and Margolis[13], and recently Ellis and Engeland[17] have all found it convenient to construct states of ^{17}O by coupling a $p_{1/2}$ proton hole to states of ^{18}F. We can examine some of the phenomenological conjectures in terms of the ZBM wave functions for nuclei with $13 \leq A \leq 19$. Zuker[19] has already shown that these wave functions possess some striking weak-coupling properties.

To a certain extent, several of these descriptions are equivalent. Consider, for example, the $\frac{11}{2}^-$ state of ^{17}O at 7.74 MeV:

$$^{17}\mathrm{O}(\tfrac{11}{2}^- \text{ at } 7.74 \text{ MeV}) = 0.89 d^2(50)p^3 - 0.41 d^4(51)p\,,$$

$$^{18}\mathrm{F}(5^+ \text{ at } 1.13 \text{ MeV}) = 0.84 d^2(50)p^4 - 0.46 d^4(51)p^2(01)\,,$$

$$^{15}\mathrm{N(g.s.)} = 0.88 p^3 + 0.44 d^2(01)p\,,$$

$$^{16}\mathrm{O}(3^- \text{ at } 6.14 \text{ MeV}) = 0.84 p^3 d + 0.48 d^3(\tfrac{5}{2}\tfrac{1}{2})p\,.$$

As far as the main, uncorrelated part (first term in the wave functions above) is concerned

$$\begin{aligned} ^{17}\mathrm{O}(\tfrac{11}{2}^- \text{ at } 7.74 \text{ MeV}) &\cong p_{1/2}{}^{-1} \otimes {}^{18}\mathrm{F}(5^+) \\ &\cong d^2(50) \otimes {}^{15}\mathrm{N(g.s.)} \\ &\cong d \otimes {}^{16}\mathrm{O}(3^-)\,. \end{aligned}$$

However, it is obvious, when the second term is considered, that the best description is indeed

$$^{17}\mathrm{O}(\tfrac{11}{2}^- \text{ at } 7.74 \text{ MeV}) = p_{1/2}{}^{-1} \otimes {}^{18}\mathrm{F}(5^+ \text{ at } 1.13 \text{ MeV})\,.$$

Similarly,

$$\begin{aligned} ^{17}\mathrm{O}(\tfrac{9}{2}^- \text{ at } 9.06 \text{ MeV}) &= -[0.83 d^2(50)p^3 \\ &\quad -0.37 d^4(51)p + 0.30 d^2(41)p^3] \\ &\cong p_{1/2}{}^{-1} \otimes {}^{18}\mathrm{F}(5^+ \text{ at } 1.13 \text{ MeV})\,. \end{aligned}$$

In Table VII we give several other examples of the successful application of the weak-coupling idea to states in ^{17}O. *A posteriori* these examples justify our having neglected the correlated part of the ^{15}N(g.s.) wave function (and renormalizing the ^{17}O wave functions for this neglect) for the purposes of DWBA analysis.

In summary, in this paper we have attempted to shed light on the 2p-1h nature of negative-parity states in ^{17}O. We have shown that our results, taken together with the results of the ^{13}C(^{7}Li, t) experiments, which provide insight into the (4p-3h) components of these states, lead to a fairly complete description of negative-parity states in ^{17}O. We find that the wave functions of ZBM provide a good description of most of the states below 9-MeV excitation. We have also shown that the success of a

direct-interaction study such as ours owes largely to the fact that many ^{17}O negative-parity states do lend themselves to a weak-coupling interpretation.

ACKNOWLEDGMENTS

We would like to thank J. L. Girma and the operating staff of the tandem Van de Graaff for their assistance during the experiment. We are indebted to L. Bianchi for help in operation of the spectrograph and to J. N. Scheurer for help in scanning the photographic plates. We would also like to thank Dr. A. P. Zuker for his interest in this work and for many stimulating discussions, and Dr. B. H. Wildenthal for communicating his unpublished results. One of us (K.K.S.) would also like to thank Dr. A. Messiah and Dr. E. Cotton for their kind hospitality during the year of his stay at CEN de Saclay.

---

*Permanent address.

[1]K. K. Seth, G. Walter, P. D. Miller, J. A. Biggerstaff, and G. R. Satchler, ORNL Physics Division Annual Report No. ORNL-3778, 1965 (unpublished), p. 104; Bull. Am. Phys. Soc. 10, 10 (1965).

[2]K. K. Seth, in *Proceedings of the Symposium on ^{3}He Induced Reactions, Saitama, Japan, 1967* (Institute of Physical and Chemical Research, Saitama, Japan, 1967), pp. 180–228.

[3]J. Cerny, private communication to K. K. Seth.

[4]K. Bethge, D. J. Pullen, and R. Middleton, Bull. Am. Phys. Soc. 13, 1464 (1968).

[5]B. G. Harvey, J. Cerny, R. M. Pehl, and E. Rivet, Nucl. Phys. 39, 160 (1962).

[6]E. Rivet, R. H. Pehl, J. Cerny, and B. G. Harvey, Phys. Rev. 141, 1021 (1966).

[7]C. C. Lu, M. S. Zisman, and B. G. Harvey, Phys. Rev. 186, 1086 (1969).

[8]I. M. Naqib and L. L. Green, Nucl. Phys. A112, 76 (1968).

[9]C. H. Johnson and J. L. Fowler, Phys. Rev. 162, 890 (1967); Phys. Rev. C 2, 124 (1970).

[10]R. F. Christy and W. A. Fowler, Phys. Rev. 96, 851 (1954).

[11]M. Harvey, Phys. Letters 3, 209 (1963).

[12]G. Ripka, in *Proceedings of the International Congress on Nuclear Physics, Paris, 1964,* edited by P. Gugenberger (Centre National de la Recherche Scientifique, Paris, France, 1964), Vol. 2, p. 360.

[13]B. Margolis and N. de Takacsy, Can. J. Phys. 44, 1431 (1966).

[14]G. E. Brown, in *Proceedings of the International Congress on Nuclear Physics, Paris, 1964* (see Ref. 12), Vol. 1, p. 142.

[15]G. E. Brown and A. M. Green, Nucl. Phys. 75, 401 (1966).

[16]A. P. Shukla, Princeton University Report No. PUC 937-262, 1966 (unpublished).

[17]P. J. Ellis and T. Engeland, Nucl. Phys. A144, 161 (1970).

[18]A. P. Zuker, B. Buck, and J. B. McGrory, Phys. Rev. Letters 21, 39 (1968).

[19]A. P. Zuker, Phys. Rev. Letters 23, 983 (1969).

[20]A. P. Zuker, B. Buck, and J. B. McGrory, Brookhaven National Laboratory Informal Report No. BNL-14085, 1969 (unpublished).

[21]B. H. Wildenthal and J. B. McGrory, private communication to K. K. Seth.

[22]J. Bobker, Phys. Rev. 185, 1294 (1969).

[23]C. P. Browne, Phys. Rev. 108, 1007 (1957).

[24]D. B. Fossan, R. L. Walter, W. E. Wilson, and H. H. Barschall, Phys. Rev. 123, 209 (1961).

[25]J. C. Davis and P. T. Noda, Nucl. Phys. A134, 361 (1969). As a consequence of this precision experiment, all energies above $E^* = 8.9$ MeV reported in Ref. 24 have been increased by 10 keV.

[26]T. W. Bonner, A. A. Kraus, J. B. Marion, and J. P. Schiffer, Phys. Rev. 102, 1348 (1956); R. L. Becker and H. H. Barschall, *ibid.* 102, 1384 (1956); M. G. Rusbridge, Proc. Phys. Soc. (London) A69, 830 (1956); J. P. Schiffer, A. A. Kraus, and J. R. Risser, Phys. Rev. 105, 1811 (1957); R. B. Walton, J. D. Clement, and F. Boreli, *ibid.* 107, 1065 (1957); B. K. Barnes, T. A. Belote, and J. R. Risser, *ibid.* 140, B616 (1965).

[27]G. W. Kerr, J. M. Morris, and J. R. Risser, Nucl. Phys. A110, 637 (1968); A. D. Robb, W. A. Schier, and E. Sheldon, *ibid.* A147, 423 (1970).

[28]W. L. Baker, C. E. Busch, J. A. Keane, and T. R. Donoghue, Phys. Rev. C 3, 494 (1970).

[29]R. H. Spear, J. D. Larson, and J. D. Pearson, Nucl. Phys. 41, 353 (1963).

[30]D. W. Heikkinen, Phys. Rev. 141, 1007 (1961); M. Meier-Ewert, K. Bethge, and K. O. Pfeiffer, Nucl. Phys. A110, 142 (1968).

[31]K. Bethge, D. J. Pullen, and R. Middleton, Phys. Rev. C 2, 395 (1970).

[32]H. Schmidt, Max Planck Institute Annual Report, Heidelberg, 1969 (unpublished), p. 84.

[33]H. B. Burrows and C. F. Powell, Proc. Roy. Soc. (London) A209, 478 (1951).

[34]C. A. Barnes, E. G. Alderberger, D. G. Hensley, and A. B. McDonald, in *Proceedings of the International Conference on Nuclear Physics, Gatlinburg, Tennessee, 12–17 September 1966,* edited by R. L. Becker and A. Zucker (Academic, New York, 1967), p. 884.

[35]C. Detraz and H. H. Duhm, Phys. Letters 29B, 29 (1969).

[36]F. G. Perey and C. M. Perey, Phys. Rev. 132, 755 (1963).

[37]K. P. Artemov, V. Z. Goldberg, B. I. Islamov, V. P. Rudakov, and I. N. Serikov, Yadern. Phys. 1, 629 (1965) [transl.: Soviet J. Nucl. Phys. 1, 450 (1965).]

[38]N. F. Mangelson, B. G. Harvey, and N. K. Glendenning, Nucl. Phys. A119, 79 (1968).

[39]W. Bohne, H. Homeyer, H. Lettau, H. Morgenstern, and J. Scheer, Nucl. Phys. A156, 93 (1970).

[40]N. K. Glendenning, Ann. Rev. Nucl. Sci. 13, 191 (1963); Phys. Rev. 137, B102 (1965).

[41]R. H. Bassel, R. M. Drisko, and G. R. Satchler, Oak Ridge National Laboratory Report No. ORNL 3240, 1962 (unpublished).

[42]J. M. Laget, Commissariat á l'Energie Atomique, Saclay Report No. CEA-R-3572 (unpublished); J. M. Laget and J. Gastebois, Nucl. Phys. A122, 431 (1968); J. M. Laget, J. Vervier, G. Bruge, J.-M. Loiseaux, and L. Valentin, *ibid.* A125, 481 (1969).
[43]F. A. Rose, Nucl. Phys. A124, 305 (1969).

PHYSICAL REVIEW C VOLUME 5, NUMBER 2 FEBRUARY 1972

Phenomenological Analysis of the $^{12}C + ^{12}C$ Reaction

Georges J. Michaud*
Département de Physique, Université de Montréal, Montréal, Québec, Canada
and
Erich W. Vogt†
Physics Department, University of British Columbia, Vancouver, British Columbia, Canada
(Received 24 June 1971)

The total $^{12}C + ^{12}C$ low-energy reaction cross section has been reanalyzed. Three phenomena suggest an α-particle model for the reaction: (1) the giant resonances, (2) the intermediate-structure resonances, and (3) anomalous branching ratios. The energy dependence of the total cross section over the energy range 2.4 to 9.0 MeV cannot be explained solely by the energy dependence of the penetration of the Coulomb barrier. There is some nuclear structure. The structure can be explained by an optical potential based on the α model leading to absorption under the barrier. It could also be explained with two giant resonances in a Woods-Saxon potential. The intermediate structure is explained as due to special states of ^{24}Mg built of a ^{12}C core and three α particles, and so are the anomalous branching ratios.

Astrophysical reaction rates were calculated for a number of possible optical potentials. The giant resonances affect the extrapolation to the energies of astrophysical interest and lead to an uncertainty of a factor of 3 to 10 in the astrophysical reaction rate at $T_9 \simeq 0.6$, where $T_9 \equiv 10^{-9} T°K$.

I. INTRODUCTION

The low-energy reactions of the $^{12}C + ^{12}C$ system have long been a fertile field for new ideas on nuclear structure. This fact and the importance of these reactions for astrophysics have sparked a continued effort to understand these reactions experimentally and theoretically. Most recently some measurements of Patterson, Winkler, and Zaidins[1] of the total absorption cross sections at energies far below the Coulomb barrier and of some branching ratios at similar energies measured by Stephens and Mazarakis[2] have added to the data, but raised new problems in the interpretation of the reaction mechanisms. In this paper, we discuss some of the questions raised by the measurements which rule out a number of conventional interpretations, and we show, phenomenologically, how the recent measurements combined with old ones lead to a picture in which the reaction is described in terms of intermediate structure in an α-particle model. In a subsequent paper we shall derive the model for the reactions in terms of known α-α interactions.

The energy region of interest here is shown in Fig. 1. Throughout this paper, all energies are in the center of mass system, unless otherwise specified. It is at energies of the $^{12}C + ^{12}C$ system from 2.5 (well below the top of the Coulomb barrier) to 9 MeV (slightly above the top of the Coulomb barrier). This corresponds to excitation energies of the compound nucleus ^{24}Mg in the neighborhood of 20 MeV.

For a well-behaved heavy-ion interaction the dominant feature of the total reaction cross section would be a plummeting cross-section magnitude as the energy decreases and the Coulomb-barrier penetration takes effect; the dominant behavior of branching ratios would be given by the statistical averages of an evaporation model. But the $^{12}C + ^{12}C$ reaction is richer and more puzzling. The total cross section plummets, as it must; but it also exhibits an unusual resonance structure in most of its reaction channels. A structure first noted 10 years ago[3] as a few isolated resonances at moderate energies was analyzed as single-particle states of the heavy-ion system in a series of papers,[4-8] but, was recently[1,2] found to extend to many more resonances at very low energies. The resonances are easily shown, as demonstrated below, to be neither single compound-nucleus states nor statistical fluctuations: On the other hand, the